NATIONAL AERONAUTICS AND SPACE ADMINISTRATION

NASA Program Apollo Working Paper No. 1347

LOW ONSET-RATE ENERGY ABSORBER

MANNED SPACECRAFT CENTER
HOUSTON, TEXAS

June 25, 1969

NASA PROGRAM APOLLO WORKING PAPER NO. 1347

LOW ONSET-RATE ENERGY ABSORBER

PREPARED BY

William H. Keathley
William H. Keathley
Spacecraft Design Office

Clarence J. Wesselski
Clarence J. Wesselski
Spacecraft Design Office

AUTHORIZED FOR DISTRIBUTION

Warren Gillespie, Jr.
for Maxime A. Faget
Director of Engineering and Development

NATIONAL AERONAUTICS AND SPACE ADMINISTRATION
MANNED SPACECRAFT CENTER
HOUSTON, TEXAS
JUNE 25, 1969

CONTENTS

FIGURES

LOW ONSET-RATE ENERGY ABSORBER

By William H. Keathley and Clarence J. Wesselski

SUMMARY

This report covers the development of a low onset-rate energy absorber to be used with the existing Apollo command-module couch struts. The energy absorber uses friction as a direct means of converting the energy to heat and achieves the low onset rate by applying the load in many small stages. Detailed information is included to permit construction of similar models for other possible applications. When this device is used, a mass moving at 28 ft/sec (19.1 mph) may be brought to rest within 18 inches at a maximum g load of 14 and an onset rate of 350 g/sec.

INTRODUCTION

A low onset-rate energy absorber has been developed for use in the Apollo command-module couch struts. The basic cyclic strut is retained in its present form, but its energy absorbing capacity is reduced to compensate for the addition of the low onset-rate device to be described here. The basic strut consists of an inner cylinder, an outer cylinder, and a series of bracelets. The bracelets are located between the inner and the outer cylinders and are made up of many small rings. When the strut is stroked, one cylinder moves axially with respect to the other, causing the small rings to roll and deflect, and thereby absorbing energy. The basic strut capacity is reduced by removing some of the bracelets.

A disadvantage of the cyclic strut is that the total load for which it was designed is applied in a very short period of time which results in excessive onset rates being applied to the couch. The problem is further aggravated by the crewmen not being firmly "seated" in the couch when this high onset rate is applied, thus resulting in an apparent (or real) amplification of g loads felt by the crewmen. By retaining only a portion of the cyclic strut and by adding a low onset-rate portion, the same energy may be absorbed while applying an acceptable g level and onset rate to the crewmen.

The major objective of this report is to prove that the concept can be used as a workable and reliable energy absorbing device.

SYMBOLS

A	acceleration (constant), ft/sec^2
A(t),B(t)	functions of time
A_c	area of contact, in^2
a	inside radius of washer, as manufactured, in.
a'.	inside radius of washer when installed on the rod, in.
a"	inside radius of washer when removed from the rod, in.
BHN	Brinnel hardness number
b	outside radius of washer, in.
C	factor equal to $c\rho$
c	specific heat, $Btu\text{-}lb_m^{-1}\text{-}{}^\circ F^{-1}$
E	modulus of elasticity, psi
E_1,$E_{1,2}$	absorbed energy, in-lb
F	stroking force, lb
$\overline{F}$	average stroking force, lb
$\overline{Fn}$	normal force, lb
$\overline{f}$	average stroking force per washer, lb
g	acceleration due to gravity, 32.2 ft/sec^2
H	drop height, in.
h	thickness of washer, in.
K	thermal conductivity, $Btu\text{-}hr^{-1}\text{-}ft^{-1}\text{-}{}^\circ F^{-1}$
L	value equal to b-a, in.
N	number of washers

$\overline{P}$	average load of ramp, lb
p	pressure, psi
q(t)	heat input per unit area
$q_o(t)$	heat output per unit area
R	factor equal to 1/K
s	stroke, in.
t	time, sec
$\overline{V}$	average stroking velocity, ft/sec
V_0	initial velocity, ft/sec
W	drop weight, lb
x	displacement of the drop weight on drop weight B
y	displacement of the drop table on drop weight B
α	factor equal to $-FA/2A_c$
β	factor equal to $FV_0/2A_c$
δ_s	washer springback equal to a"-a', in.
ε	strain of material, in/in. or percent
$\theta(0,t)$	surface temperature over ambient temperature of washer at inside diametrical surface, ^oF
μ	coefficient of friction
ν	Poisson's ratio
ρ	density, lb_m/in^3
σ	stress, psi
ϕ	functional symbol

Operators:

($\dot{}$) velocity, ft/sec

($\ddot{}$) acceleration, ft/sec^2

TEST ARTICLE DESCRIPTION

The low onset-rate energy absorber consists of a rod and a series of washers. The washers are pressed onto a rod and spaced some distance apart as shown in figures 1 and 2. The couch energy is absorbed by stroking the washers along the rod. Because the washers are picked up one at a time, the total load is realized only after the strut has stroked some significant distance. By varying the spacing of the washers, the onset rate can be controlled. Similarly, the load can be controlled by the number of washers installed.

(a) Before stroking (0.080-inch spacing).

Figure 1.- Rod and washer assembly.

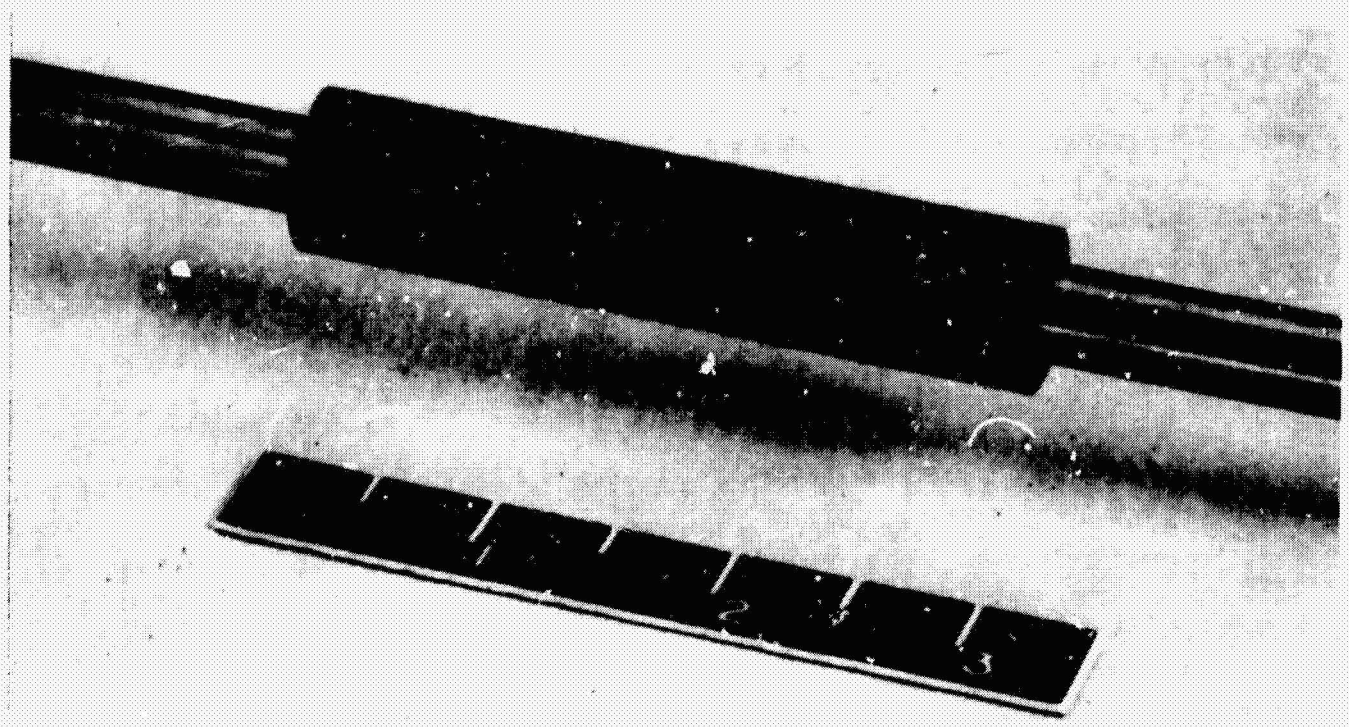

(b) After stroking.

Figure 1.- Concluded.

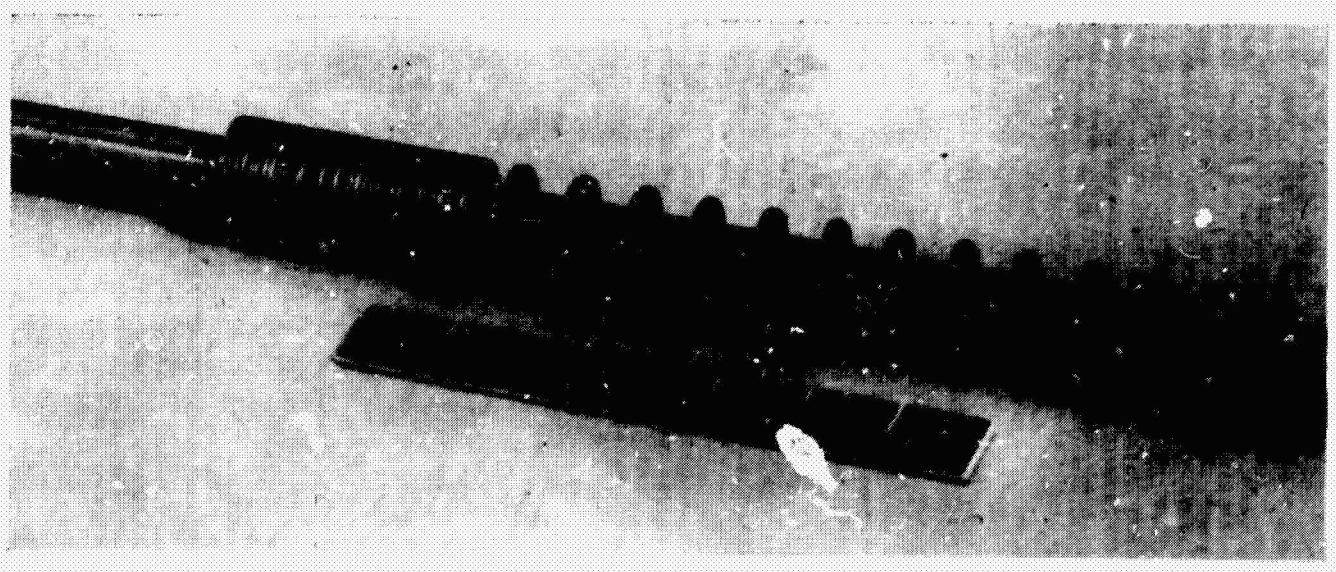

Figure 2.- Partially stroked rod and washer assembly (0.32-inch spacing).

The rod diameter may be 0.375 ± 0 0005 inch, but the variation in the diameter of a particular rod from one end to the other must not vary more than 0.0001 inch in order to maintain a uniform load. The surface of the rod must have an 8 to 16 microinch finish and must be hard relative to the washers. A taper of approximately one-fourth in/ft was provided at one end for washer installation. Drill rod, 17-4 PH stainless steel, and 718 inconel were tested for possible use as rod materials. Both the drill rod and the stainless steel tended to gall at velocities below the desired level of 25 ft/sec, but the inconel showed no signs of galling at velocities as high as 28 ft/sec. All tests using the inconel rods were made on rods having a hardness of 40 Rockwell C.

The washers are also rather special because the final load-stroke curve is dependent upon the characteristics of each individual washer. Many materials were considered, but only two were tested, 304 and 416 stainless steel. The 304 stainless steel was discarded because of the high coefficient of expansion. The washers were machined from process-annealed bar stock, and the faces were surface ground. Tolerances were maintained all over at ±0.001 inch. The inside diameter of the washer was machined 0.010 inch smaller than the diameter of the rod. When the washer is pressed onto the rod, the 0.010 inch interference causes the washer to yield, making it conform exactly to the rod without the necessity for extremely close tolerances on the parts. The rod, then, becomes a sizing mandrel and causes each washer to offer the same resistance to sliding. The washer thickness selected for this application was 0.040 inch and was the only thickness tested. Analysis indicates that the load would be a linear function of the thickness but this has not been verified by test. The outside diameter of the washer was selected to limit the bearing stress to approximately one-half the material yield strength.

After all machining was completed, the washers were fully annealed in an inert gas atmosphere. Full annealing of 416 stainless steel requires that the material be held at 1600° F for 1 hour, followed by cooling at a rate no faster than 50° F per hour to 1100° F. The material may then be cooled at a faster rate, but care must be taken to ensure that the material does not come in contact with air until room temperature is reached. Contact with air at elevated temperatures will cause heavy oxidation and scaling. Both of these conditions will cause variations in the loads the washers will produce.

HARDNESS TESTING

The relationship between the hardness of the washers and the load on the rod produced by the washers may be determined directly by hardness readings made on a diamond penetrant machine (for example, a Vickers or Microtron hardness tester). Other types of hardness testers

were found to produce erratic results, and the hardness did not correlate with the calculated loads or test loads. To determine the average load that a rod-washer configuration will produce, the diamond penetrant hardness (DPH) number should be converted to Rockwell B (R_B) or Brinnel hardness numbers, and the average force should be determined from the washer load chart (fig. 3). It should be noted that this chart deals only with average loads and average velocities. An arbitrarily selected point on a test curve cannot be used to predict loads because the load is dependent on the coefficient of friction; the coefficient of friction is in turn dependent on the heating rate. It naturally follows that a load at a given point is dependent on what has transpired before that point is reached. Thus, loads should be determined from the chart based on the energy to be absorbed, the average velocity, and the available stroke.

LUBRICATION

Correct lubrication is essential for the proper operation of the rod-washer energy absorber. Several high-quality oils and greases were tested for possible use as lubricants; none of these appeared promising. Miller Stephenson dry-film lubricant MS-122 successfully produced the desired results and proved to be highly repeatable. This lubricant is contained in spray cans, and the active ingredient is tetrafluoroethylene polymer solids. It is produced by the Miller Stephenson Chemical Company, Inc., Los Angeles, California, and is covered under Military Specification MIL-L-60326 (MU) Amend. 1, Type 1.

Prior to washer installation, the rod and washers should be thoroughly clean with Freon to remove any oil or grease; the rod should not be handled after cleaning to prevent contamination by the natural oil on the hands. The rod may be handled with rubber gloves, a clean rag, or by the threaded end of the rod. The lubricant should be applied liberally to the rod prior to each washer installation, and the rod should be thoroughly sprayed again prior to installation of the rod assembly. There should be an obvious buildup of lubricant on all stroking areas of the rod.

TEST EQUIPMENT

Drop rig A (fig. 4) is a single-mass system where the drop weight is hoisted to an elevated position and then dropped. Its energy is then absorbed by the rod and washer assembly. As the weight is stroking, its negative acceleration produces the velocity-time curve shown in figure 5.

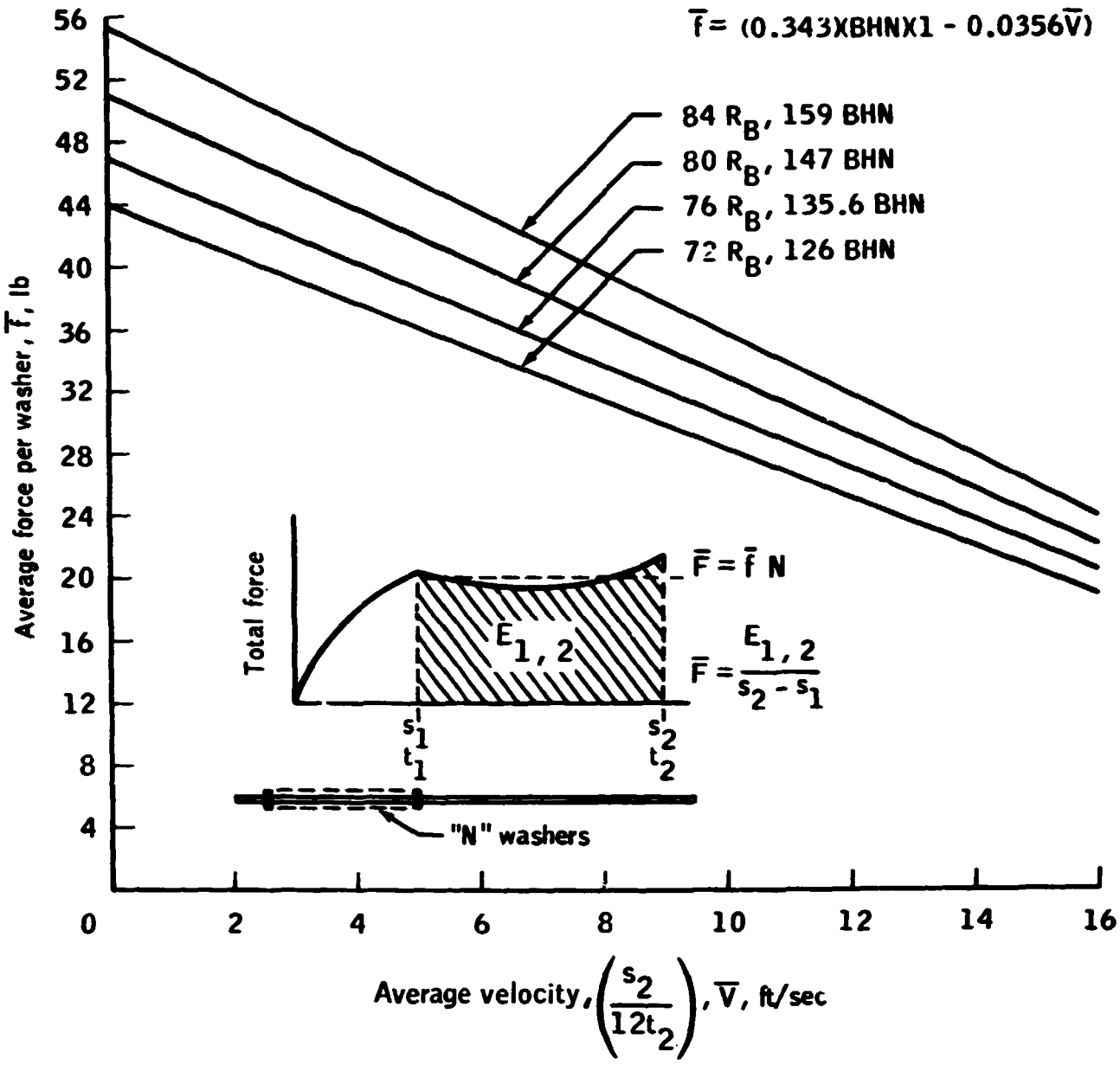

Figure 3.- Washer load chart (3/8-inch nominal).

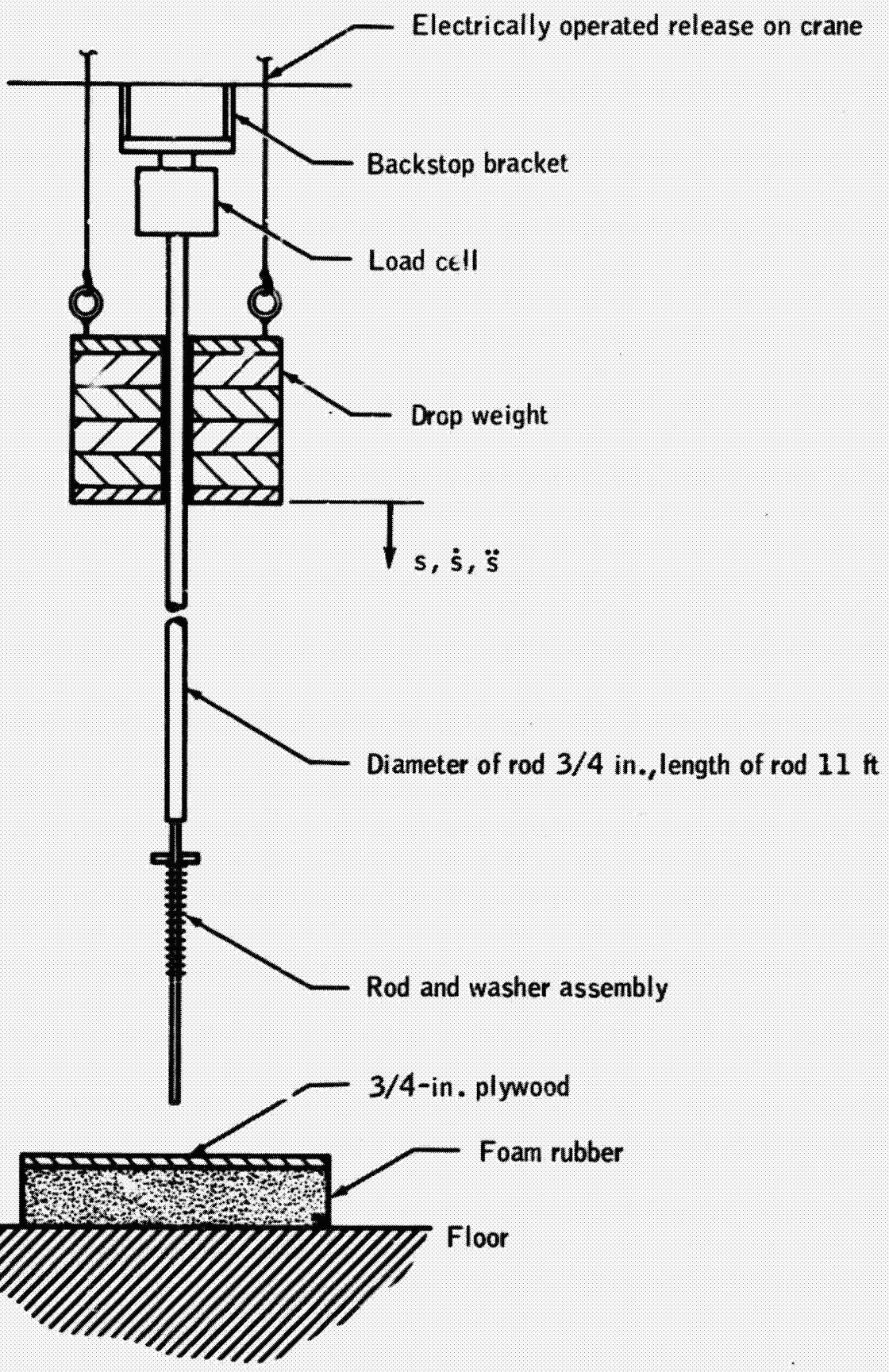

Figure 4.- Drop rig A.

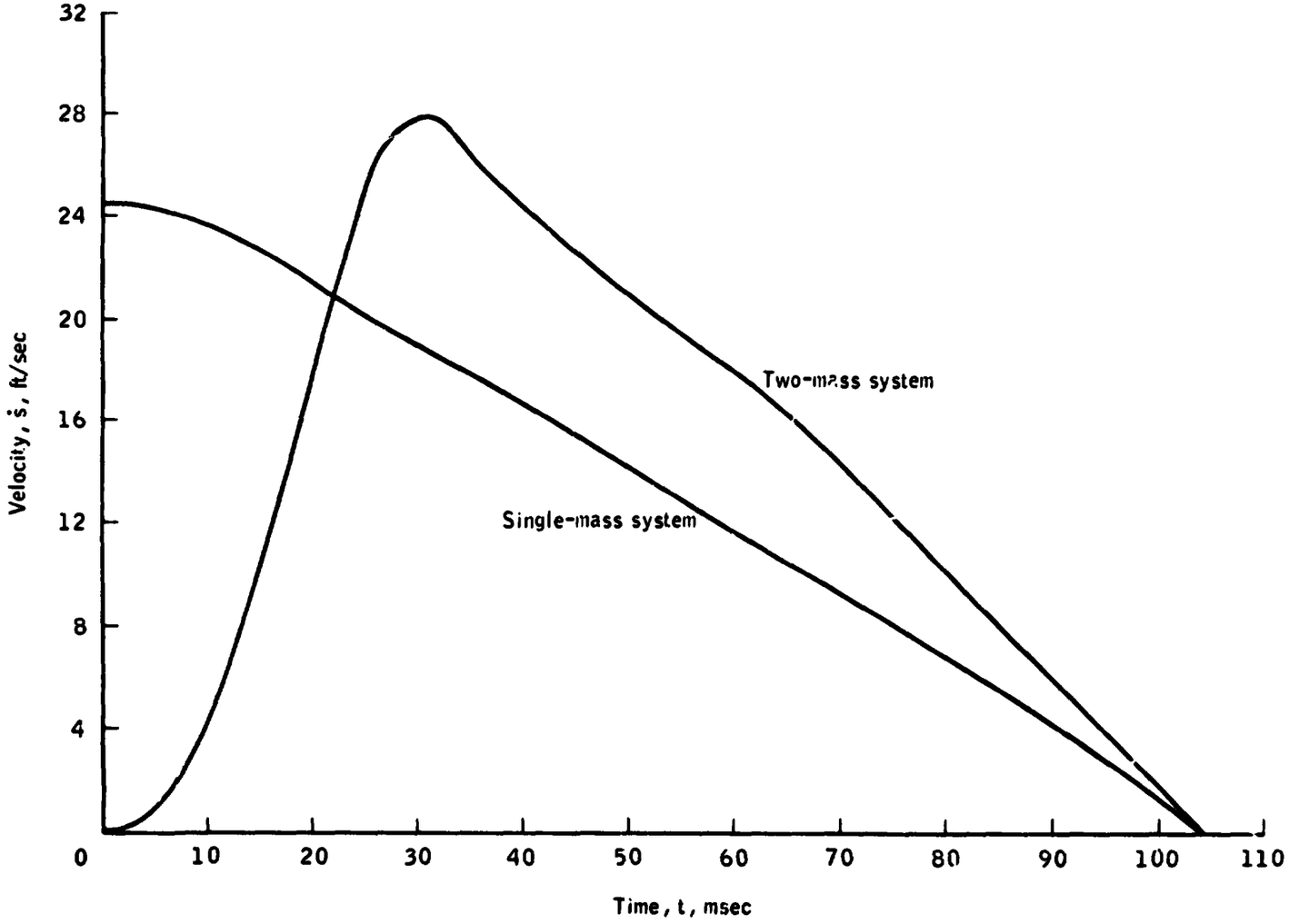

Figure 5.- Typical velocity-time curve.

The instrumentation consists of a load cell which is electrically connected to a recorder. To find the velocity and stroke as a function of time, numerical integration of the load-time curve is computed, and these equations are used.

$$\ddot{s} = g\left(1 - \frac{F}{W}\right) \tag{1}$$

$$\dot{s} = V_0 + g\left(t - \int_0^t \frac{F}{W}\, dt\right) \tag{2}$$

$$s = \int_0^t \dot{s}\, dt \tag{3}$$

Drop rig B is a two-mass system which simulates more closely the condition of a spacecraft landing. It is shown schematically in figure 6 in a "ready for drop" position. The table (approximately 5000 pounds) is considered as the first mass, and the drop weight (144 pounds) is considered as the second mass. The second mass is statically supported by the first three washers. When the release is actuated, both masses accelerate to the same initial velocity V_0.

Washer stroking then becomes a relative displacement between the two masses, and because the table ram is programed to stroke out first, the resulting stroke velocity starts at zero, rises to a peak of 28 ft/sec, and then drops to zero as shown in figure 5. The instrumentation consists of a strain gage which provides washer load and accelerometers. The accelerometers are mounted on the drop table and on the drop weight. The stroke velocity and displacement are then determined by numerical integration by using the following equations.

$$\ddot{s} = \ddot{x} - \ddot{y} \tag{4}$$

$$\dot{s} = \int_0^t (\ddot{x} - \ddot{y})dt \tag{5}$$

$$s = \int_0^t \dot{s}\, dt \tag{6}$$

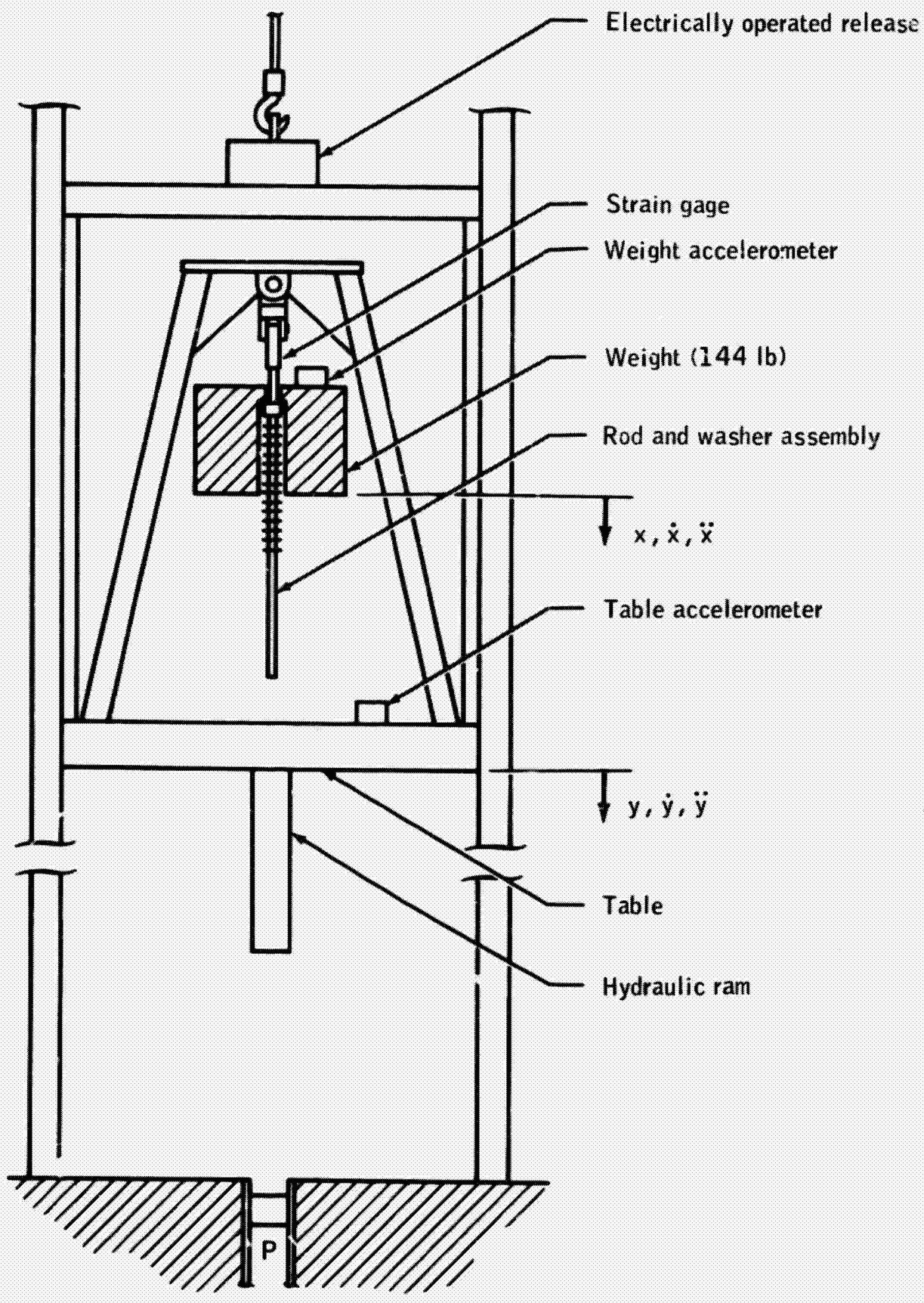

Figure 6.- Drop rig B.

ANALYSIS ON ROD AND WASHER ENERGY ABSORBER

In this portion of the report, pertinent loads, deflections, and stresses are analyzed for design purposes. Because this is a friction mechanism, a rigorous mathematical solution to the problem is not needed at this time. Any additional accuracy gained probably would be offset by the difference between the assumed and the actual coefficient of friction. The contact pressure, the stroking load on the washer, the washer springback, the tensile stress in the rod, and the surface temperatures will be determined in the following section. There are two underlying features of this friction mechanism which will be discussed briefly to perform the analysis.

Boundary Lubrication

Lubricated sliding surfaces fall into two categories. The first category is hydrodynamic (or thick-film) lubrication in which ideally the surfaces never touch. The friction falls within the range of $\mu = 0.001$ to 0.0001; no wear occurs. The second category is boundary (or thin-film) lubrication in which the high points on the surfaces touch. The friction falls within the range of $\mu = 0.05$ to 0.15; some wear occurs. The latter condition occurs when the pressure between the contact surfaces becomes so great that the lubricant film cannot support the load. In view of the above criteria, it is obvious that boundary lubrication is the most applicable to this friction mechanism. When the lubricant and the materials are chosen, the coefficient of friction usually falls in a much narrower range as long as severe wear (galling, seizing, etc.) does not occur. It is assumed that some wear is normal under boundary lubrication conditions, but it should not be visible to the eye; severe wear is abnormal and visible.

Plastic Deformation of the Washer

The washer is made with an inside diameter which is 2-1/2 percent smaller than the rod size. Because the elastic limit on the strain is approximately 0.1 percent, the entire washer is deformed plastically when it is driven on the shaft. The 2-1/2 percent strain will not rupture the washer when it is fully annealed because the ultimate strain is approximately 30 percent. This feature minimizes the effect of manufacturing tolerances, which otherwise would have to be considered in the analysis.

Stroking Load on Washer

In considering the deformation of the washer beyond the elastic limit, it is assumed that the material is perfectly plastic, that is, the material follows Hooke's law up to the proportional limit and then yields under a constant stress without strain hardening. The stress-strain curve for an assumed perfectly plastic material is shown in figure 7. Figure 8 illustrates a thick-walled cylinder yielding under the action of an internal pressure. The solution to this problem has already been determined because it is applicable to the autofrettage process in making gun barrels. The pressure required to bring the entire washer into the plastic flow state (ref. 1) is

$$p = \sigma_y \log_e \frac{b}{a} \tag{7}$$

When the washer is installed on the rod (fig. 9), the contact area is

$$A_c = 2\pi a' h \tag{8}$$

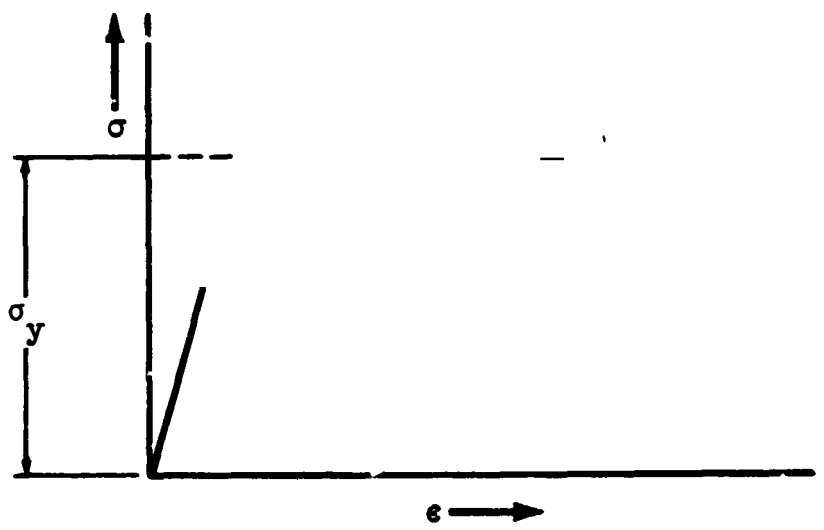

Figure 7.- Stress-strain curve for an assumed perfectly plastic material.

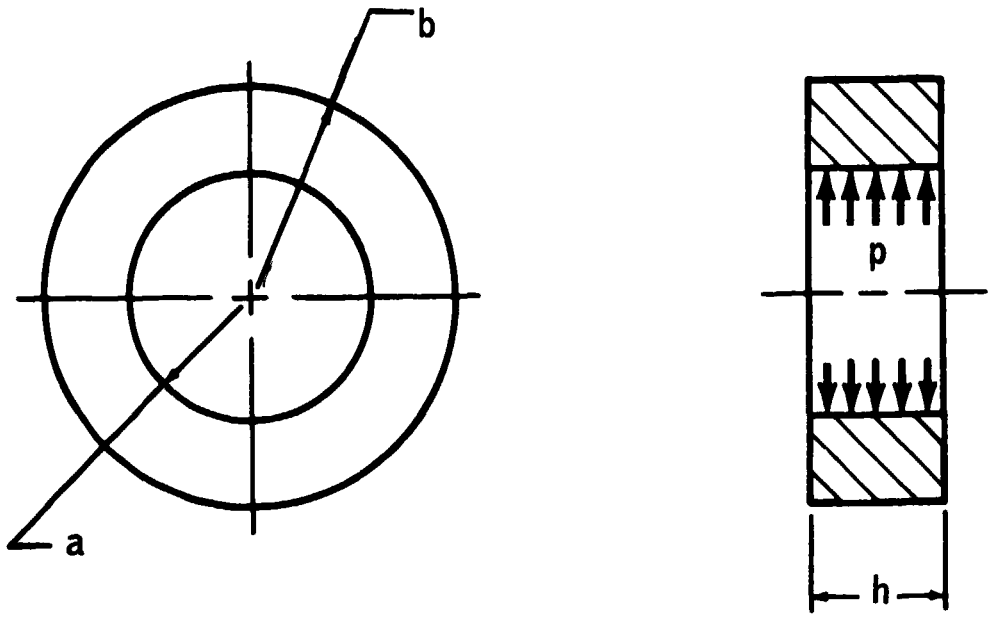

Figure 8.- Washer geometry, as manufactured.

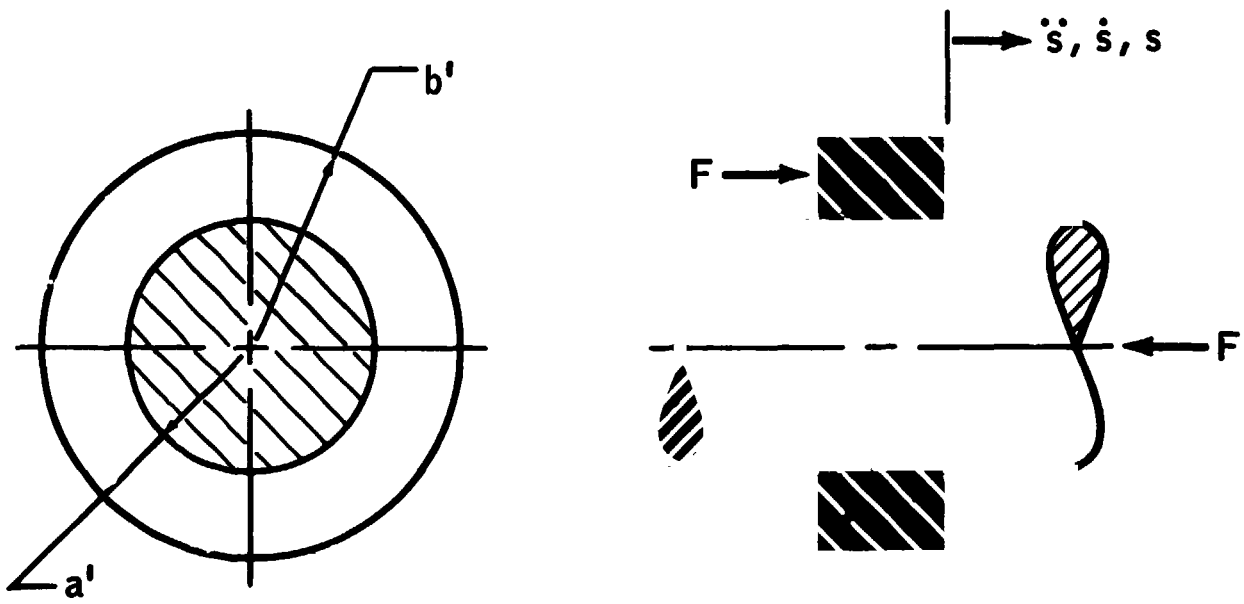

Figure 9.- Washer and rod geometry.

The force required to stroke the washer along the rod is

$$F = \mu p A_c \tag{9}$$

Substitute the values $a = 0.183$, $b = 0.3125$, $a' = 0.1875$, $h = 0.040$, and $\sigma_y = 40\ 000$ psi into equations (7) to (9) to obtain

$$p = 40\ 000 \log_e \frac{0.3125}{0.183} = 21\ 400 \text{ psi}$$

$$A_c = 2(0.1875)(0.040) = 0.0471 \text{ in}^2$$

$$F = \mu(21\ 400)(0.0471) = \mu(1008)$$

As stated previously, boundary lubrication generally yields coefficients of friction in the range of $\mu = 0.05$ to 0.15; thus, the stroking load will be $F = 50$ to 150 pounds.

It will be shown later in the report that the load actually falls on the lowest end of the range when MS-122 lubricant is used and goes even lower with increasing stroking velocities.

Washer Springback

When the washer is removed from the rod (radius denoted as a'), the inside radius of the washer will assume a new value (new value of radius denoted as a''). The difference $\delta_s = a' - a''$ will be the amount of springback. The value is important because if the rod diameter decreases along the length in the direction of washer travel, the load will decrease and may even vanish if this variation is greater than the springback amount. During unloading, Hooke's law (ref. 2) will be used, thus

$$\delta_s = p \frac{a}{E}\left(\frac{b^2 + a^2}{b^2 - a^2} + \nu\right) \tag{10}$$

Substituting the values $p = 21\ 400$ psi, $a = 0.183$ in., $b = 0.3125$ in., $\nu = 0.3$, and $E = 29 \times 10^6$ psi into equation (10) will yield

$$\delta_s = \frac{21\ 400(0.183)}{29 \times 10^6}\left(\frac{0.3125^2 + 0.183^2}{0.3125^2 - 0.183^2} + 0.3\right) = 0.00032 \text{ in.}$$

Therefore, if the rod diameter decreases 0.00064 inch, the load will vanish. The maximum allowable variation of rod diameter in manufacturing is 0.0001 inch.

Tensile Stress in Rod

For a 3/8-inch rod with a 3/8-24 UNF thread on one end, the minimum diameter is 0.324 inch. The cross-sectional area is then 0.0823 in^2. For an applied load of 2000 pounds, an assumed stress concentration factor of 2.0, and a load amplification factor of 2.0, the stress is

$$\sigma = \frac{(2000)(2)(2)}{0.0823} = 97\ 000 \text{ psi}$$

Because the rod material is 718 inconel, which has a yield strength of 174 000 psi, the rod is strong enough.

Surface Temperatures

The purpose of this section is to determine how the surface temperature varies with displacement or time as the washer strokes along the rod. A simplified friction and heat model will be used as shown in figure 10. If it is assumed that 50 percent of the heat goes into the sliding block and the friction force is constant, the heat transfer rate per unit area of contact is

$$q(t) = \frac{1}{2} \frac{F\dot{s}}{A_c} \tag{11}$$

If a constant acceleration is used, the sliding velocity and displacement is

$$\ddot{s} = A, \text{ constant} \tag{12}$$

$$\dot{s} = V_0 + At \tag{13}$$

$$s = V_0 t + \frac{1}{2} At^2 \tag{14}$$

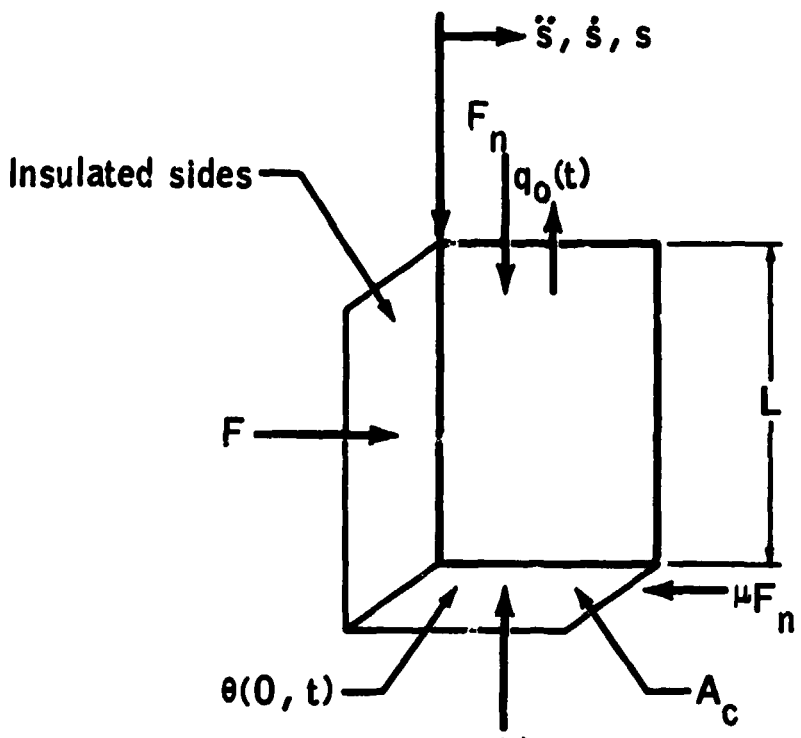

Figure 10.- Friction and heat model.

Substitute equation (13) into equation (11) to obtain

$$q(t) = \frac{1}{2}\frac{F}{A_c}\left(V_0 + At\right) \tag{15}$$

or

$$q(t) = \beta - \alpha t \tag{16}$$

where $\beta = FV_0/2A_c$ and $\alpha = -Fa/2A_c$. (17)

The solution to the heat-diffusion partial-differential equation for surface temperature (ref. 3) is

$$\theta(0,t) = \beta\sqrt{\frac{R}{C}}\left(\frac{t}{L\sqrt{RC}} + \frac{L\sqrt{RC}}{3} - \frac{2L\sqrt{RC}}{\pi^2}\sum_{n=1}^{\infty}\frac{1}{n^2}e^{-\frac{n^2\pi^2}{L^2RC}t}\right) - \alpha\sqrt{\frac{R}{C}}\left(\frac{t^2}{2L\sqrt{RC}} + \frac{L\sqrt{RC}}{3} - \frac{L^3(RC)^{3/2}}{45} + \frac{2L^3(RC)^{3/2}}{\pi^4}\sum_{n=1}^{\infty}\frac{1}{n^4}e^{-\frac{n^2\pi^2}{L^2RC}t}\right) \tag{18}$$

The properties of 416 stainless steel are $c = 0.11$ Btu-lb_m^{-1}-$°F^{-1}$, $K = 15$ Btu-hr^{-1}-ft^{-1}-$°F^{-1}$, and $\rho = 0.28$ lb_m-in^{-3}. When these values and $L = 1/8$ in. are substituted into equation (18), the surface temperature is

$$\theta(0,t) = \beta\left(27.778t + 12.875 - 7.827\sum_{n-1}^{\infty}\frac{1}{n^2}e^{-7.098n^2t}\right) - \alpha\left(13.889t^2 + 12.875t - 1.1935 + 1.1027\sum_{n=1}^{\infty}\frac{1}{n^4}e^{-7.098n^2t}\right) \tag{19}$$

$$\theta(0,t) = \beta B(t) + \alpha A(t) \tag{20}$$

where β must have the units Kip-in^{-1}-sec^{-1} and α must have the units Kip-in^{-1}-sec^{-2}. A tabulation of the functions of B(t) and A(t) for the range $0 < t \leq 0.10$ sec is given as follows.

t	B(t)	A(t)
0	0	0
.01	3.6947	.0247
.02	5.2263	.0696
.03	6.3995	.1281
.04	7.3911	.1973
.05	8.2590	.2761
.06	9.0644	.3606
.07	9.7750	.4569
.08	10.4519	.5578
.09	11.0827	.6659
.10	11.6876	.7794

By using an initial velocity of 25 ft/sec, the effect of acceleration on surface temperature will be determined. The velocity profiles shown in figure 11 will be used as typical test conditions. For $A_c = 0.0472$ in^2 and F = 50 lb (constant), the values of β and α are as follows.

$$\beta = \frac{50(25)}{2(0.0472)} \frac{(12)}{100} = 159 \frac{\text{Kip-in}}{\text{in}^2\text{-sec}}$$

$$\alpha = \frac{50(250)}{2(0.0472)} \frac{12}{1000} = 1590 \frac{\text{Kip-in}}{\text{in}^2\text{-sec}^2} \quad (A = -7.8g)$$

$$\alpha = -\frac{50(125)(12)}{2(0.0472)(1000)} = 795\ \frac{\text{Kip-in}}{\text{in}^2\text{-sec}^2}\ (A = -3.9g)$$

$$\alpha = 0\ (A = 0)$$

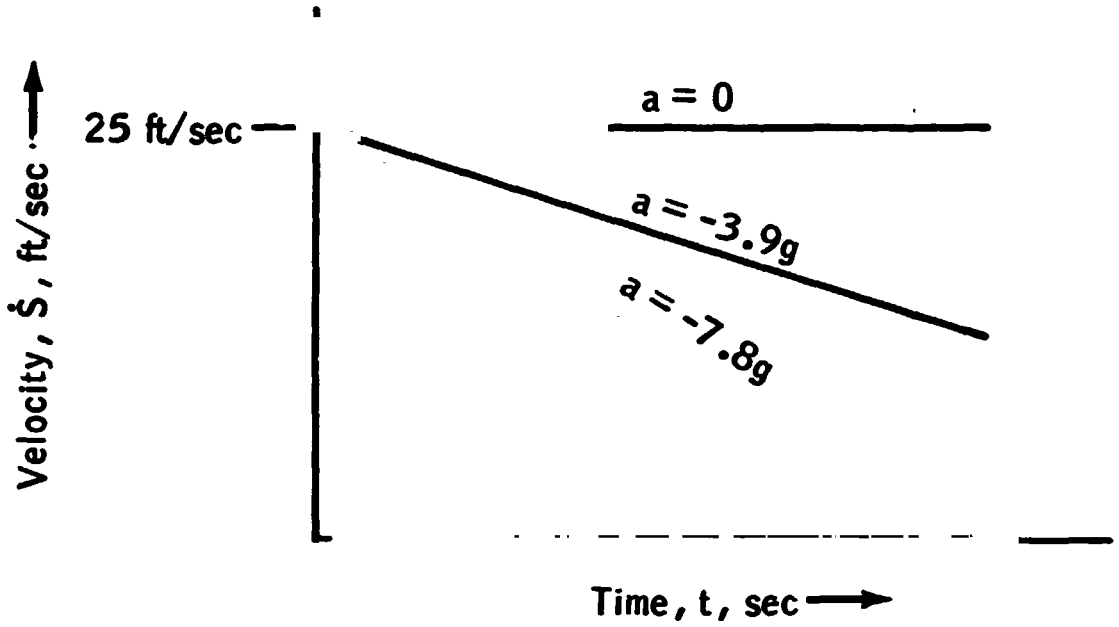

Figure 11.- Velocity profiles.

By substituting these values into equation (20) and by using the tabular values of B(t) and A(t), the temperatures versus time values can be tabulated. Then, by using equation (14), the displacements versus time values are tabulated. The temperatures are then plotted versus displacements for the three values of acceleration. These results are shown in figure 12.

TEST PROGRAM

Testing was done in two phases in this program. The first phase was a preliminary testing process. Test rig A was used to determine the feasibility of this concept and to determine the best design features (such as materials and lubricants) and preliminary design data. The results were then used as an input to the second phase of testing which was done on both test rigs. In the second phase, the design of the rod and washer assembly for a specific purpose was tested under various conditions to determine the effects on the stroking load.

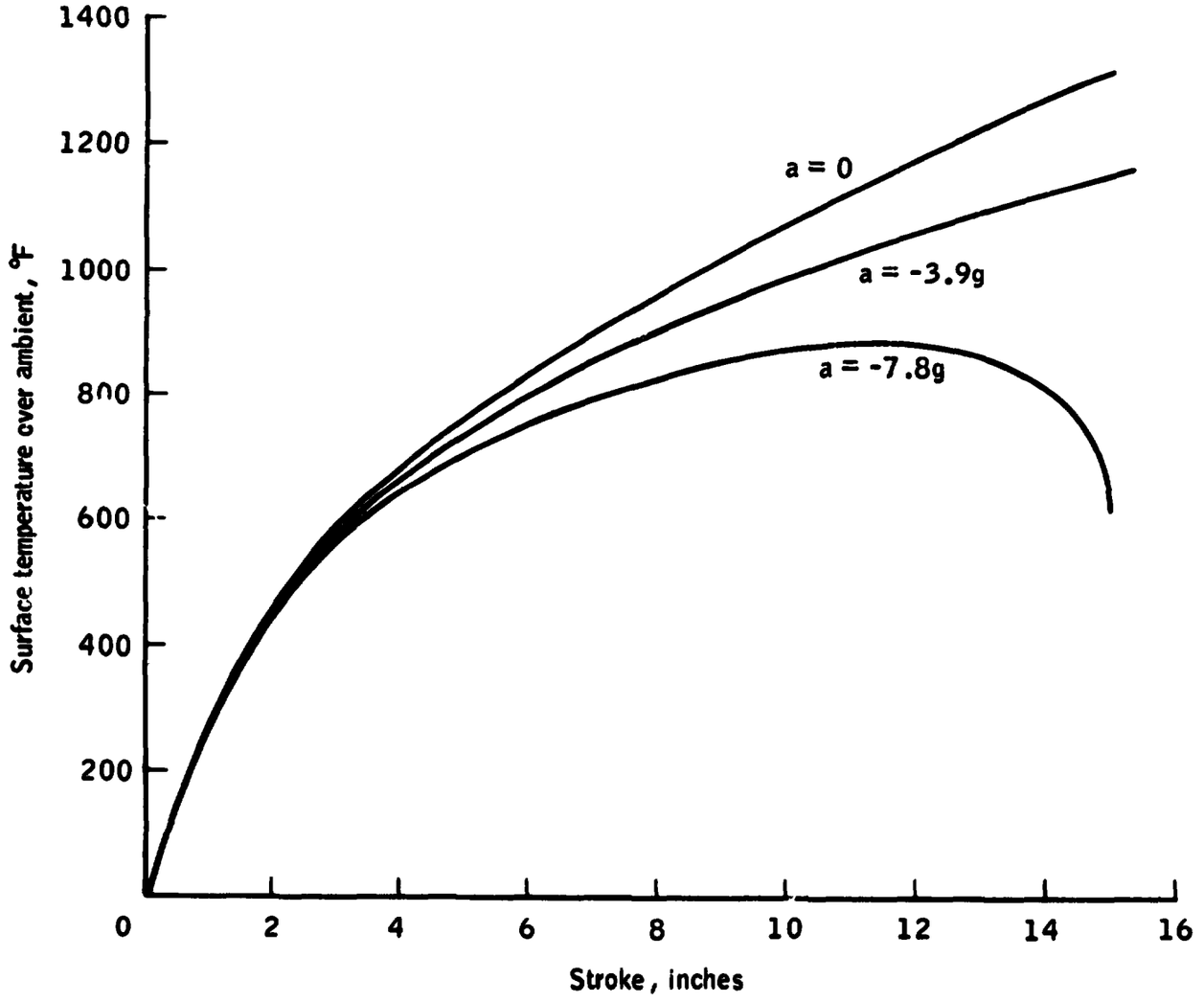

Figure 12.- Temperature as a function of stroke (V_0 = 25 ft/sec).

RESULTS AND DISCUSSION

Phase I

Materials.- As stated previously, many materials were considered but were discarded for various reasons.

The series of tests conducted on the 17-4 PH stainless steel rods and the 416 stainless steel washers showed that galling started to occur at 14 ft/sec, and severe galling occurred at 24 ft/sec even though various lubricants were tried. Therefore, 17-4 PH stainless steel was not considered any further.

The series of tests conducted on the 718 inconel rods and on the 416 stainless steel washers showed no signs of galling at velocities up to 28 ft/sec. These materials were ultimately chosen in the design.

Lubricants.- Krytox 240 AC was a Teflon grease-type lubricant which did not produce good load-time traces. The load increased excessively as the stroke velocity reached zero.

The Teflon spray-on lubricant MS-122 was found to produce better load-time traces because of its dry-film characteristics.

Phase II

After the preliminary tests were conducted to determine the best design features, several other tests were conducted. These results are given in figures 13 to 20. All the rod and washer assemblies were loaded to give the load-stroke curve shown in figure 21.

The washers, made from 416 stainless steel, were to be annealed to a nominal value of R_B 83 hardness; however, the actual hardness ranged from 76 to 79 R_B. Preliminary tests indicated that 76 washers (at R_B 83) on the rod would give approximately the desired load level of 2000 pounds at the maximum velocity range. Accordingly, all the tests had 76 washers except for test 47A which had 61. As observed on the test data, the average load was somewhat lower because the washers were softer than desired.

Six other similarities in the tests were as follows:

1. The rod material was 718 inconel.

2. The rod size was 3/8 inch.

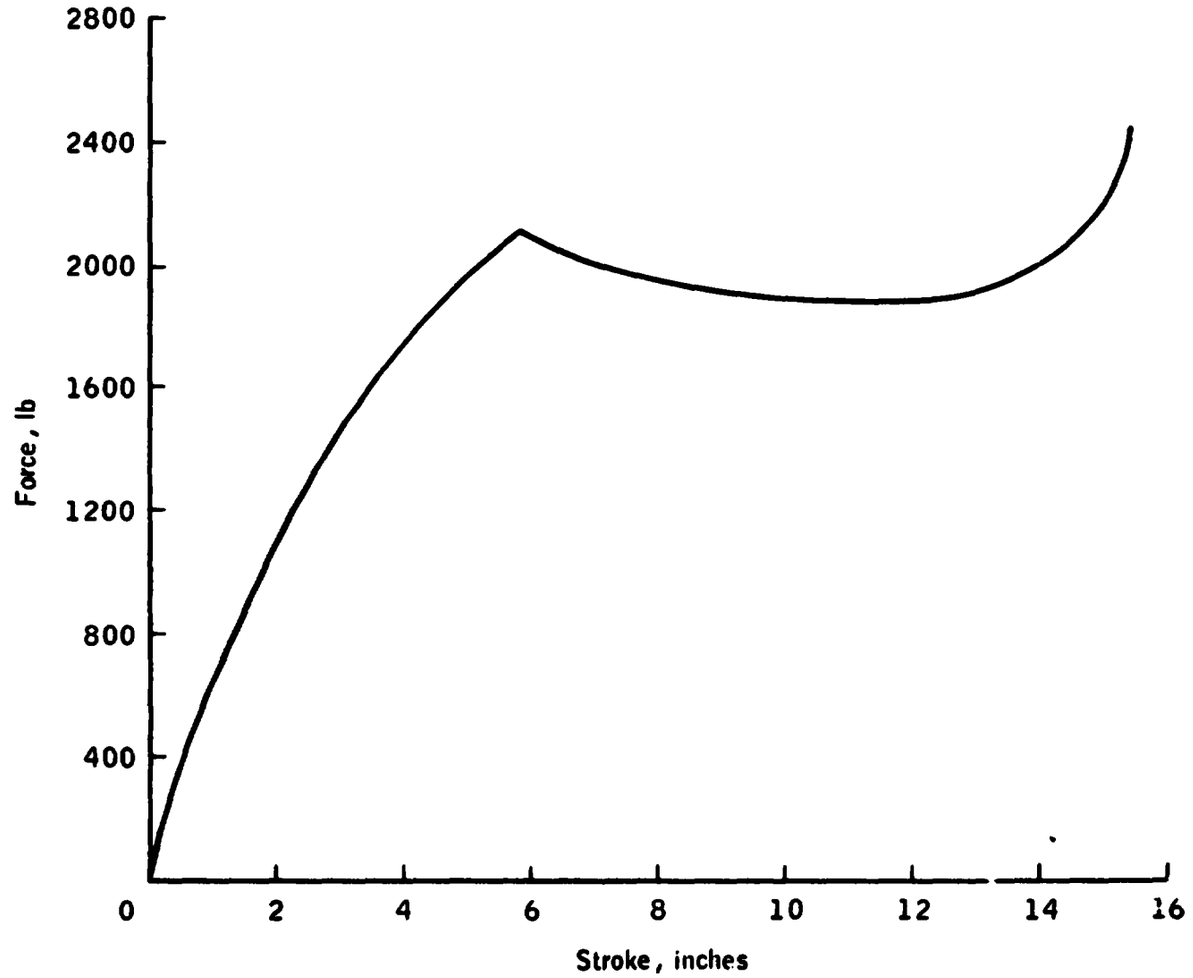

(a) Load-stroke curve.

Figure 13.- Data for test 45A.

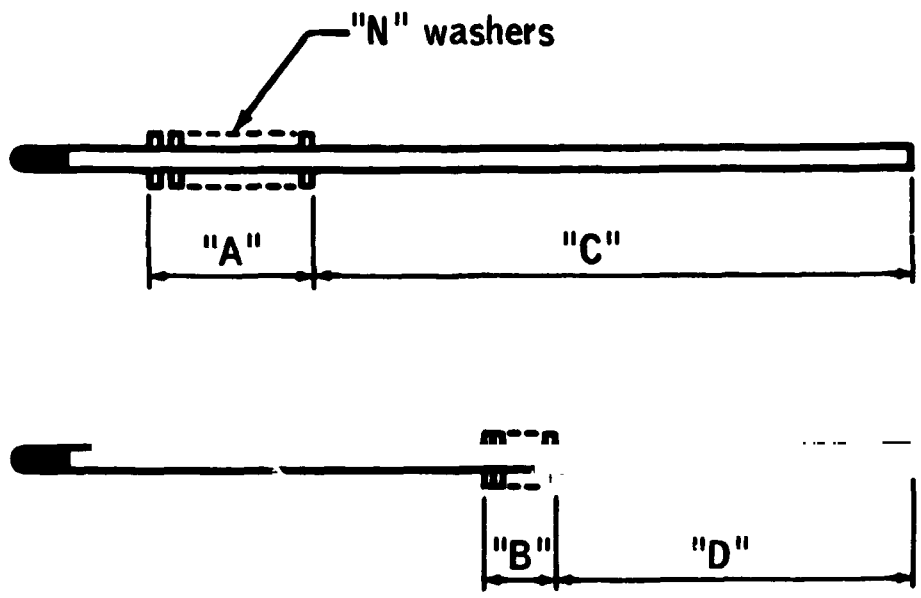

Date of test	12/4/68
Drop rig	A
Rod size, in.	3/8
Drop weight W, lb	216
Drop height H, in.	111.8
Number of washers N	76
Dimension "A," in.	8.93
Dimension "B," in.	3.04
Stroke s_1 = A-B, in.	5.89
Dimension "C," in.	18.84
Dimension "D," in.	9.23
Stroke $s_2 - s_1$ = C-D, in.	9.61
Total stroke s_2, in.	15.50
Stroke time t_1, msec	22
Stroke time t_2, msec	96
Washer hardness, R_B number	77
Force F_1, lb	2100
Force F_{min}, lb	1880
Force F_2, lb	2460

(b) Test values.

Figure 13.- Continued.

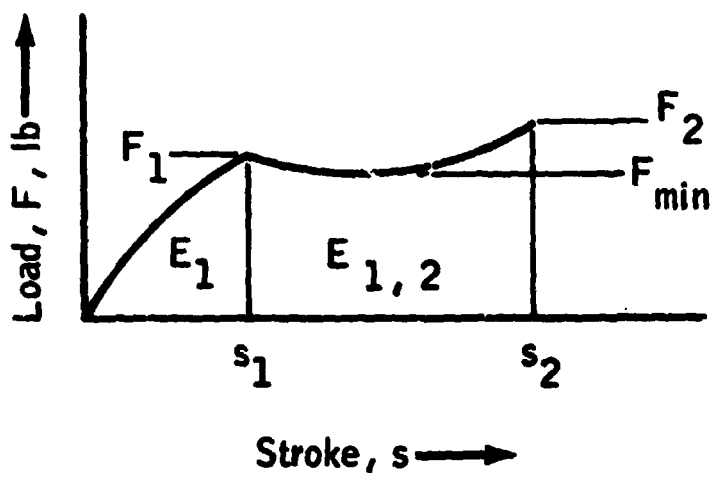

Maximum stroking velocity V_{max}, ft/sec	24.50
Stroke at $V = V_{max}$, in.	0.0
Average stroking velocity $\bar{V} = s_2/t_2$, ft/sec	13.45
Absorbed energy, $0 < s < s_1$, E_1, in-lb	8085
Average load, $0 < s < s_1$, $\bar{P}$, lb	1370
Absorbed energy, $s_1 < s < s_2$, $E_{1,2}$, in-lb	19 422
Average load, $s_1 < s < s_2$, $\bar{F}$, lb	2 020
Average load per washer, $\bar{f} = \bar{F}/N$, lb	26.6
Ratio P/F, percent	67.8
Ratio $F_1/\bar{F}$, percent	104.0
Ratio $F_{min}/\bar{F}$, percent	93.1
Ratio $F_2/\bar{F}$, percent	121.8

Remarks: This rod was not cleaned with Freon prior to installing washers.

(c) Calculated values.

Figure 13.- Concluded.

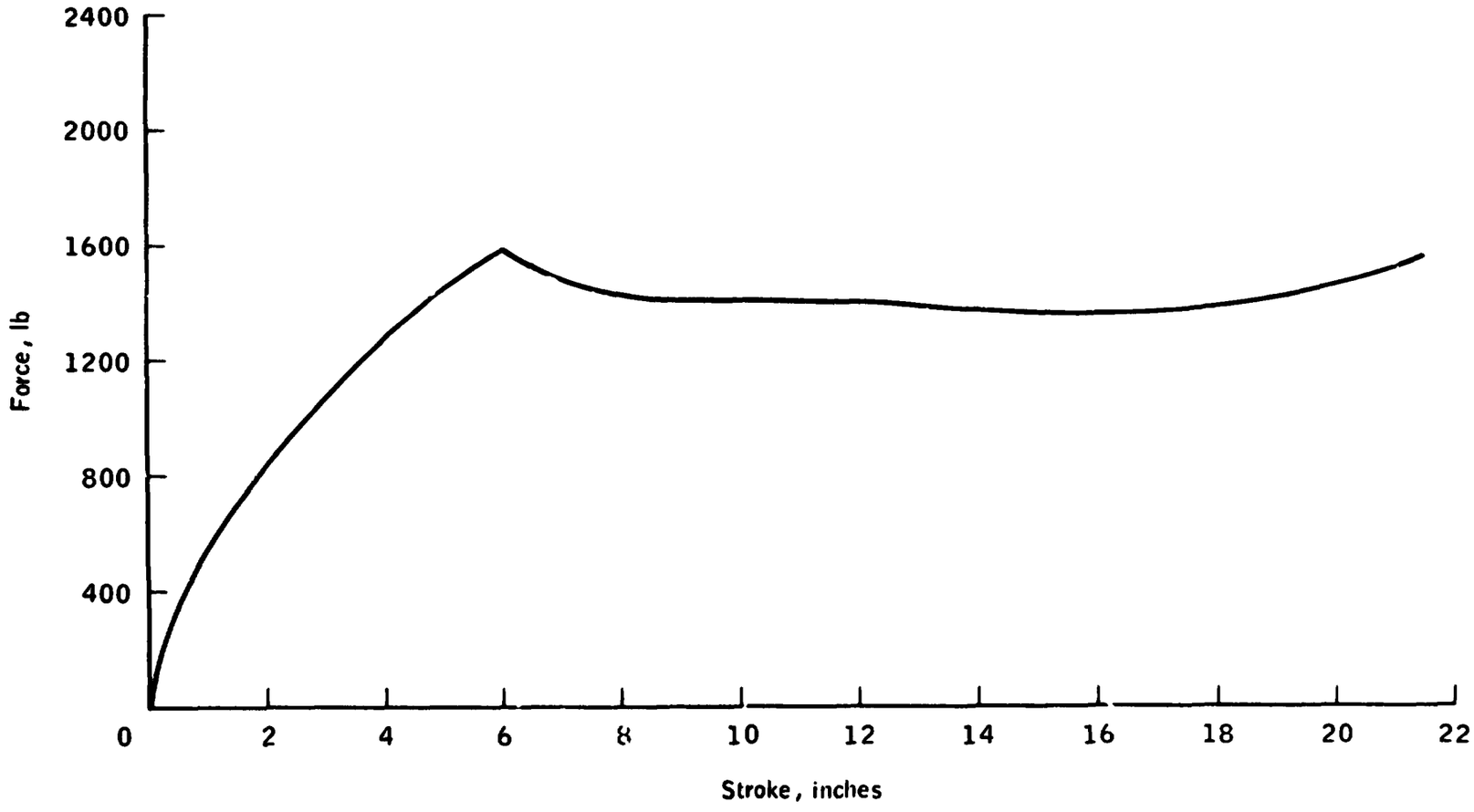

(a) Load-stroke curve.

Figure 14.- Data for test 47A.

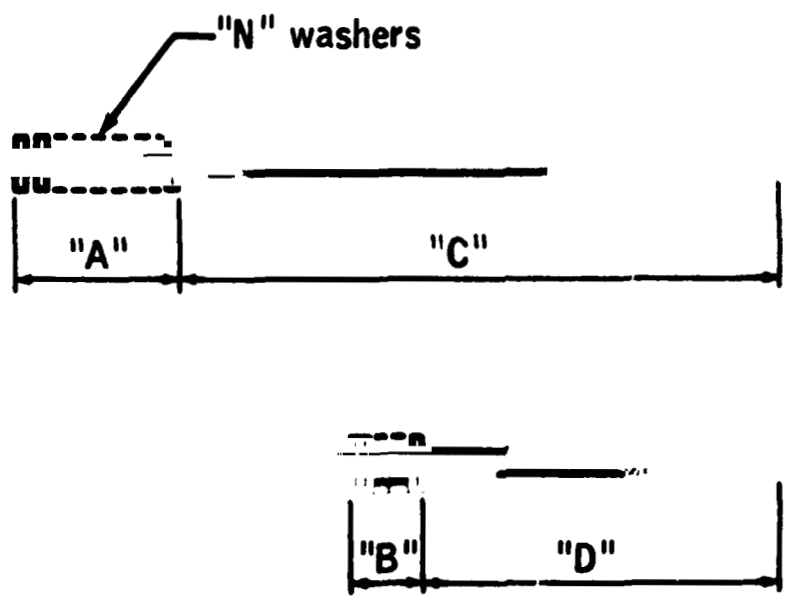

Date of test	12/10/68
Drop rig	A
Rod size, in.	3/8
Drop weight W, lb	216
Drop height H, in.	112.4
Number of washers N	61
Dimension "A," in.	8.42
Dimension "B," in.	2.44
Stroke s_1 = A-B, in.	5.98
Dimension "C," in.	19.03
Dimension "D," in.	3.40
Stroke $s_2 - s_1$ = C-D, in.	15.63
Total stroke s_2, in.	21.61
Stroke time t_1, msec	20
Stroke time t_2, msec	130
Washer hardness, R_B number	77
Force F_1, lb	1570
Force F_{min}, lb	1350
Force F_2, lb	1570

(b) Test values.

Figure 14.- Continued.

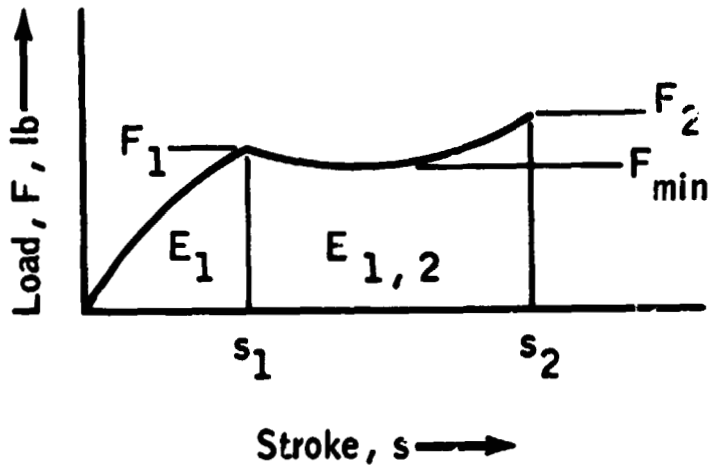

Maximum stroking velocity V_{max}, ft/sec	24.55
Stroke at $V = V_{max}$, in.	0.0
Average stroking velocity $\bar{V} = s_2/t_2$, ft/sec	13.85
Absorbed energy, $0 < s < s_1$, E_1, in-lb	5 943
Average load, $0 < s < s_1$, $\bar{P}$, lb	993
Absorbed energy, $s_1 < s < s_2$, $E_{1,2}$, in-lb	22 784
Average load, $s_1 < s < s_2$, $\bar{F}$, lb	1 457
Average load per washer, $\bar{f} = \bar{F}/N$, lb	23.8
Ratio $\bar{P}_t/\bar{F}$ percent	68.2
Ratio $F_1/\bar{F}$, percent	107.8
Ratio $F_{min}/\bar{F}$, percent	92.7
Ratio $F_2/\bar{F}$, percent	107.8

(c) Calculated values.

Figure 14.- Concluded.

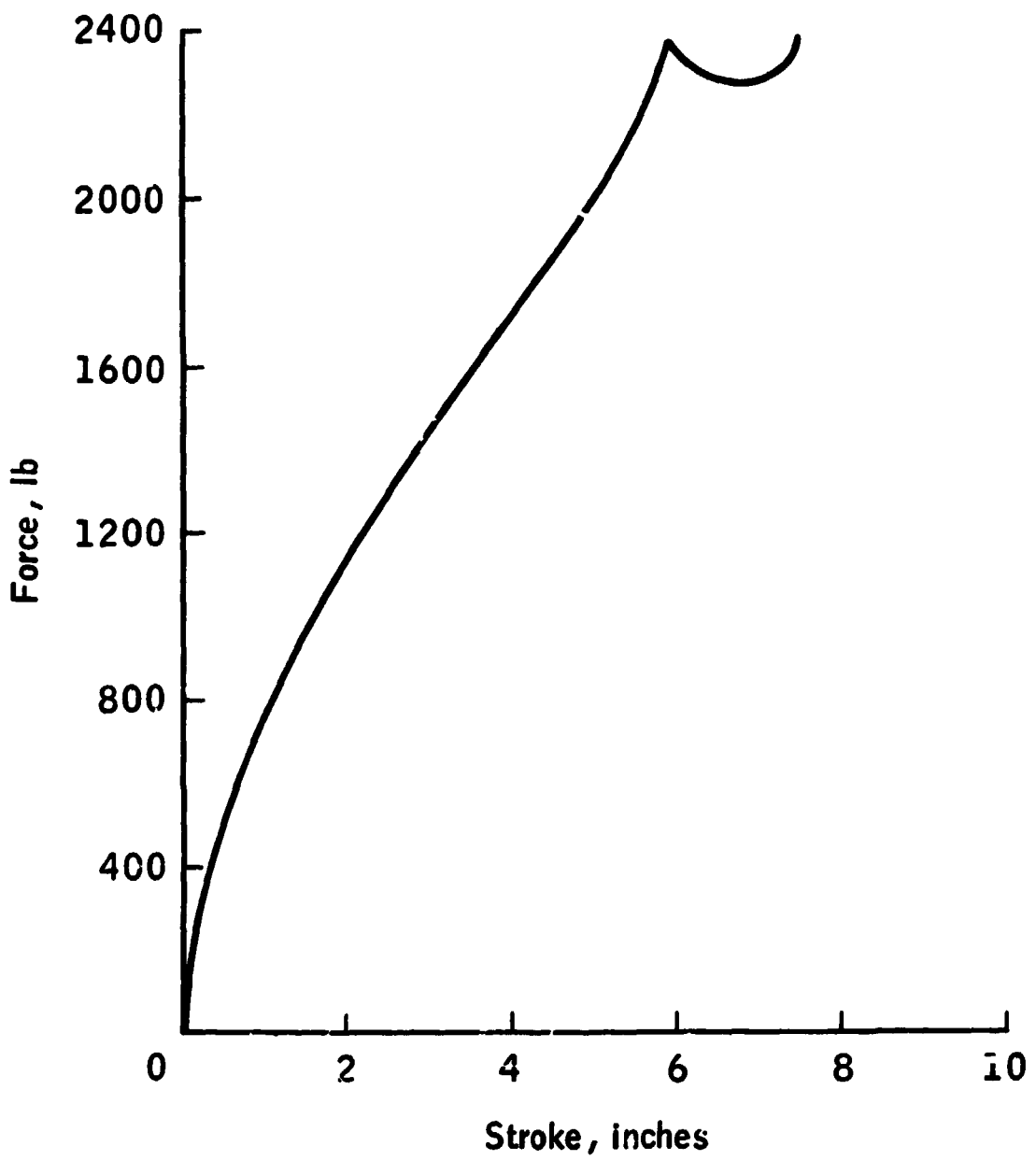

(a) Load-stroke curve.

Figure 15.- Data for test 46A.

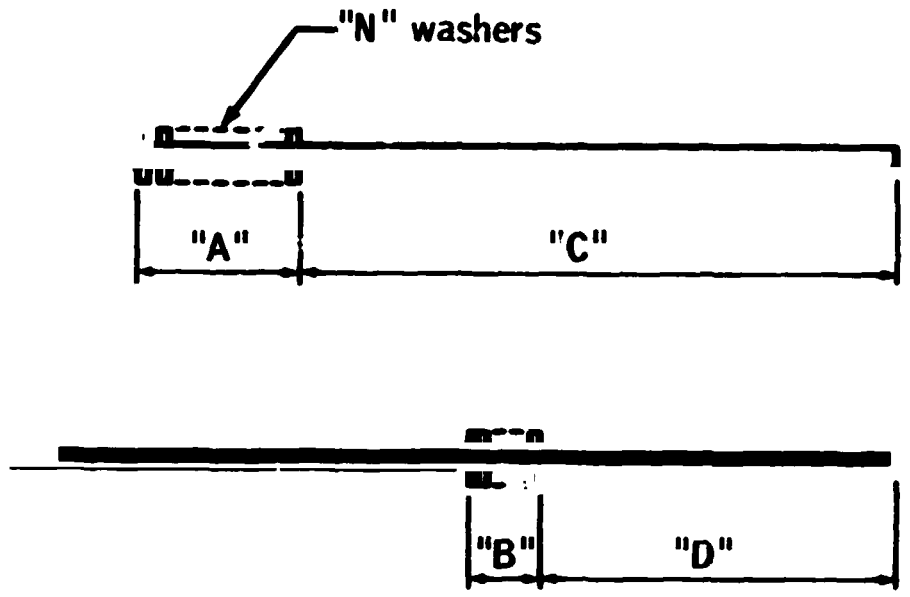

Date of test	12/12/68
Drop rig	A
Rod size, in.	3/8
Drop weight W, lb	216
Drop height H, in.	48
Number of washers N	76
Dimension "A," in.	9.00
Dimension "B," in.	3.04
Stroke s_1 = A-B, in.	5.96
Dimension "C," in.	18.44
Dimension "D," in.	16.90
Stroke $s_2 - s_1$ = C-D, in.	1.54
Total stroke s_2, in.	7.50
Stroke time t_1, msec	35
Stroke time t_2, msec	61
Washer hardness, R_B number	78
Force F_1, lb	2360
Force F_{min}, lb	2280
Force F_2, lb	2400

(b) Test values.

Figure 15.- Continued.

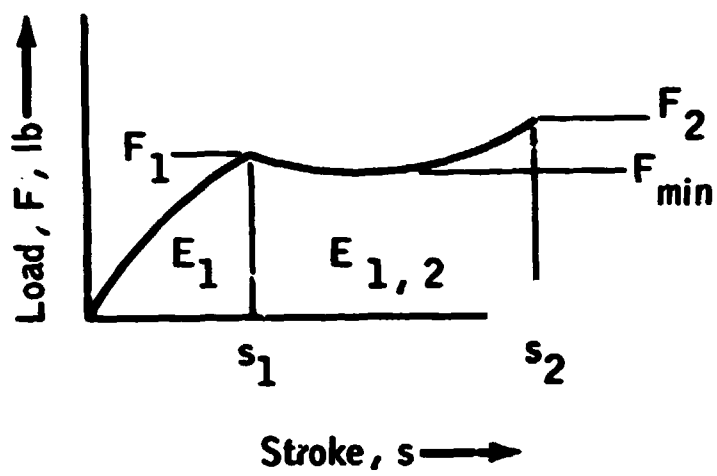

Maximum stroking velocity V_{max}, ft/sec	16.05
Stroke at $V = V_{max}$, in.	0.00
Average stroking velocity $\bar{V} = s_2/t_2$, ft/sec	10.25
Absorbed energy, $0 < s < s_1$, E_1, in-lb	8410
Average load, $0 < s < s_1$, $\bar{P}$, lb	1410
Absorbed energy, $s_1 < s < s_2$, $E_{1,2}$, in-lb	3578
Average load, $s_1 < s < s_2$, $\bar{F}$, lb	2320
Average load per washer, $\bar{f} = \bar{F}/N$, lb	30.6
Ratio $\bar{P}_t/\bar{F}$, percent	60.8
Ratio $F_1/\bar{F}$, percent	101.8
Ratio $F_{min}/\bar{F}$, percent	98.2
Ratio $F_2/\bar{F}$, percent	103.4

(c) Calculated values.

Figure 15.- Concluded.

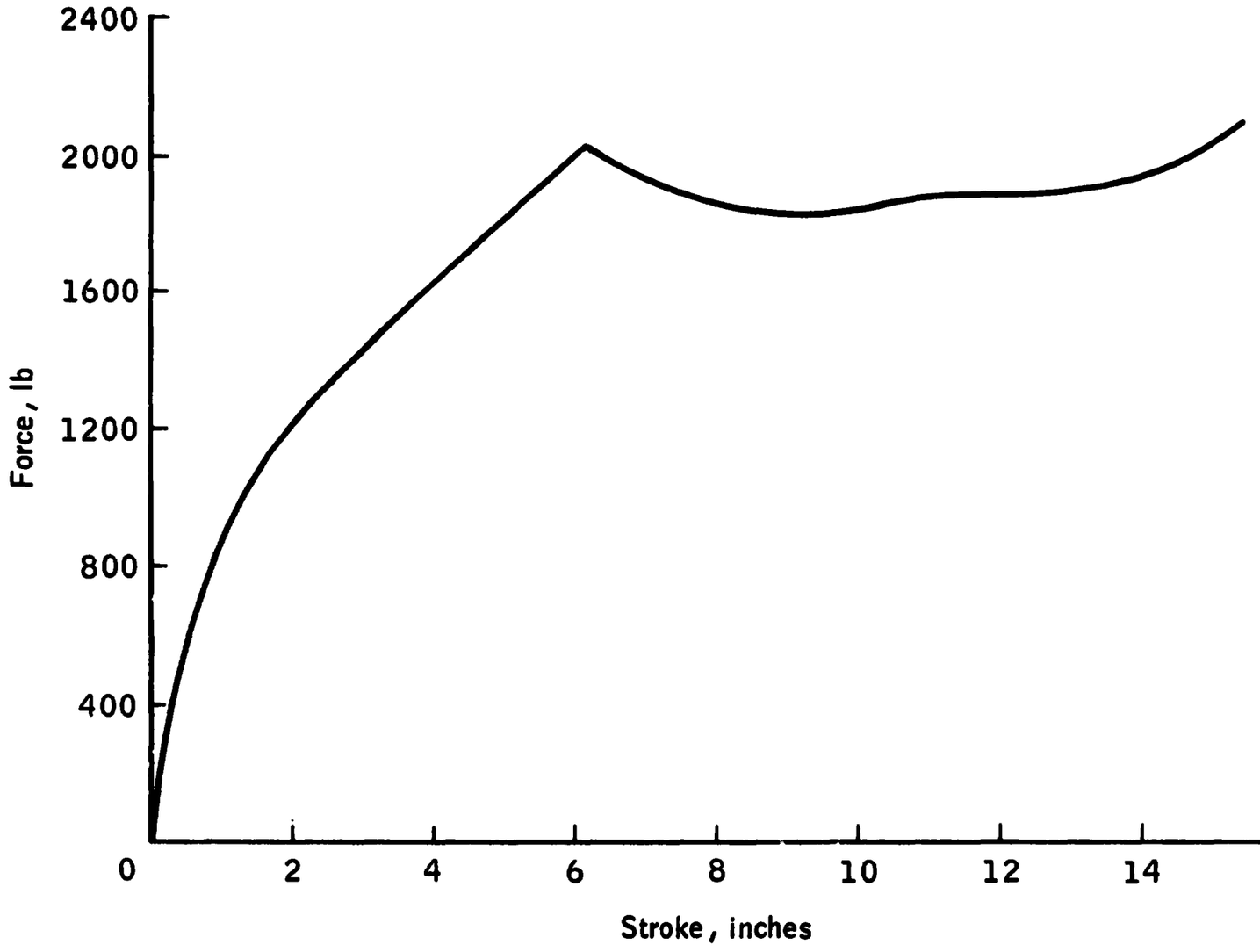

(a) Load-stroke curve.

Figure 16.- Data for test 49A.

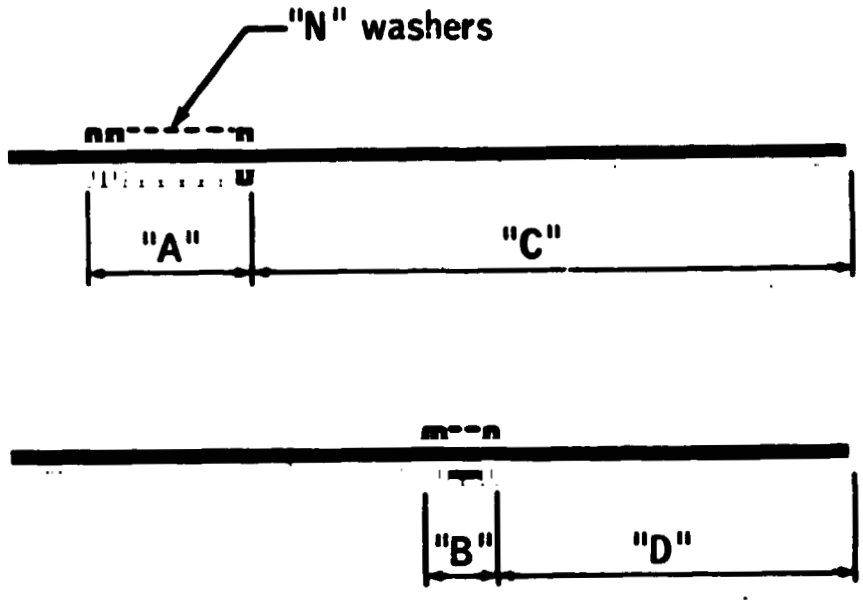

Date of test	12/13/68
Drop rig	A
Rod size, in.	3/8
Drop weight W, lb	216
Drop height H, in.	111.6
Number of washers N	76
Dimension "A," in.	9.19
Dimension "B," in.	3.04
Stroke s_1 = A-B, in.	6.15
Dimension "C," in.	18.94
Dimension "D," in.	9.63
Stroke $s_2 - s_1$ = C-D, in.	9.31
Total stroke s_2, in.	15.46
Stroke time t_1, msec	22
Stroke time t_2, msec	95
Washer hardness, R_B number	78
Force F_1, lb	2020
Force F_{min}, lb	1830
Force F_2, lb	2100

(b) Test values.

Figure 16.- Continued.

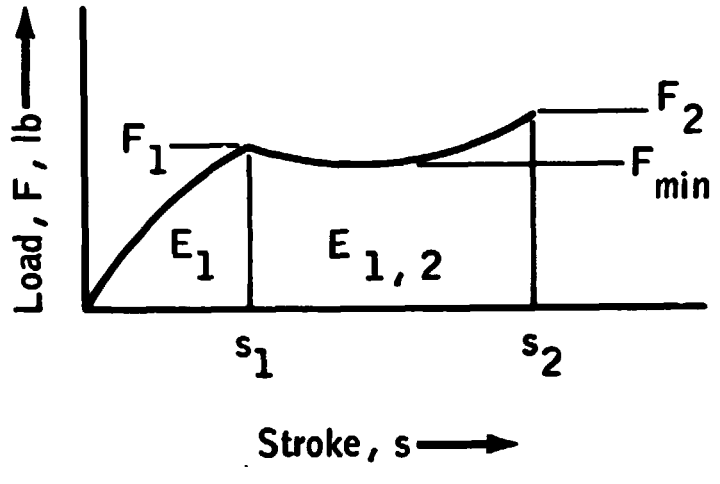

Maximum stroking velocity V_{max}, ft/sec	24.47
Stroke at $V = V_{max}$, in.	0.00
Average stroking velocity $\overline{V} = s_2/t_2$, ft/sec	13.41
Absorbed energy, $0 < s < s_1$, E_1, in-lb	8 530
Average load, $0 < s < s_1$, $\overline{P}$, lb	1 390
Absorbed energy, $s_1 < s < s_2$, $E_{1,2}$, in-lb	18 909
Average load, $s_1 < s < s_2$, $\overline{F}$, lb	2 030
Average load per washer, $\overline{f} = \overline{F}/N$, lb	26.7
Ratio $\overline{P}_t/\overline{F}$, percent	68.5
Ratio $F_1/\overline{F}$, percent	99.5
Ratio $F_{min}/\overline{F}$, percent	90.2
Ratio $F_2/\overline{F}$, percent	103.4

Remarks: The first 17 washers were oxidized on the surface.

(c) Calculated values.

Figure 16.- Concluded.

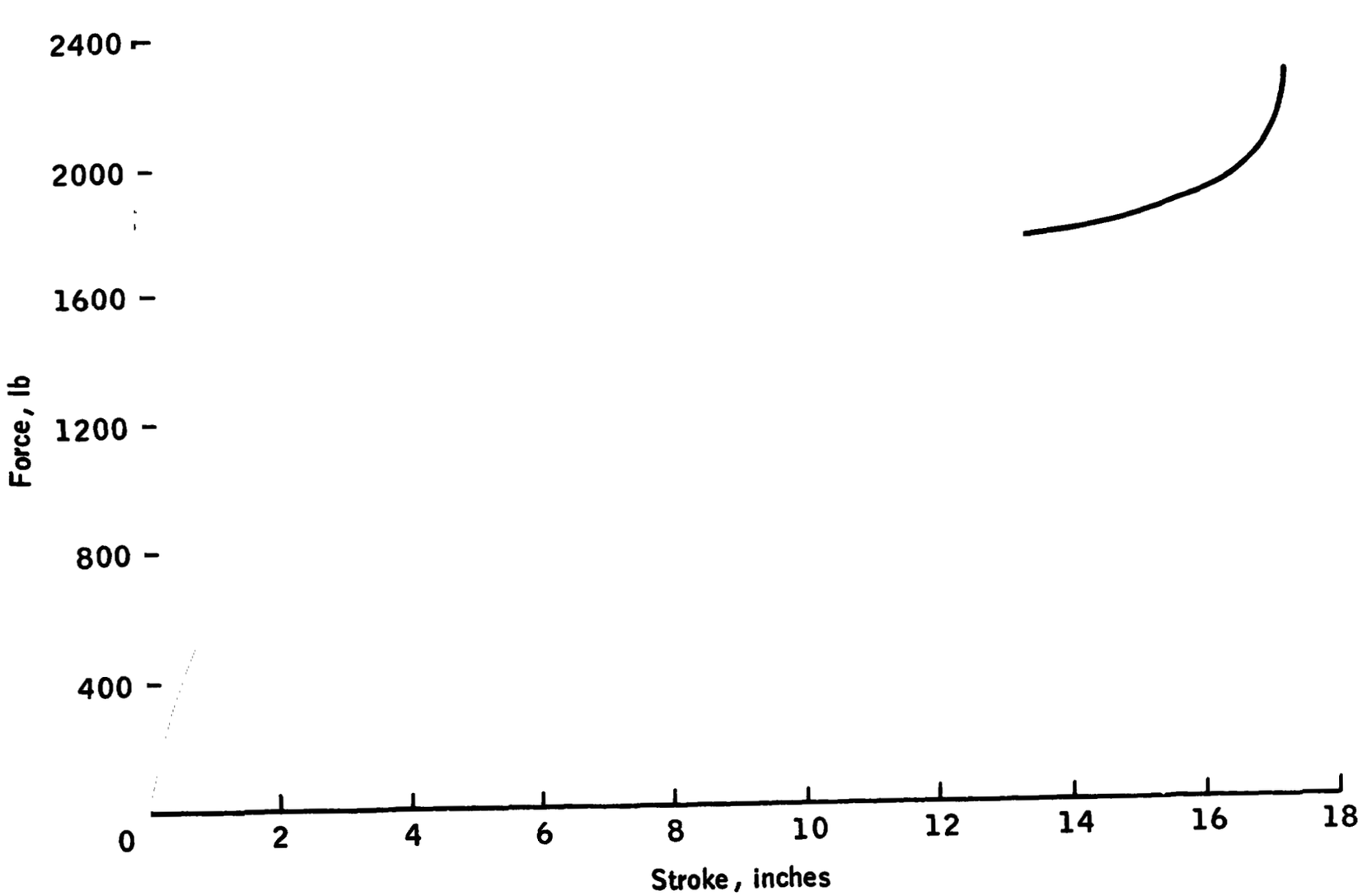

(a) Load-stroke curve.

Figure 17.- Data for test 50A.

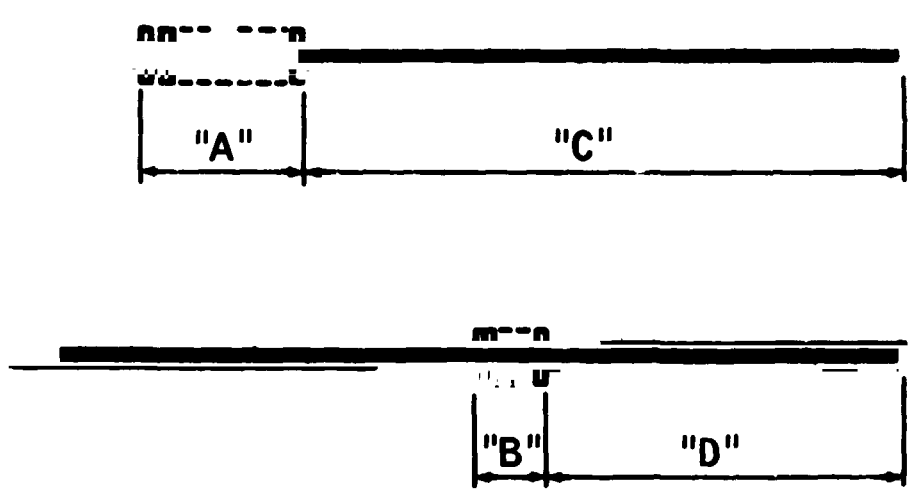

Date of test	12/16/68
Drop rig	A
Rod size, in.	3/8
Drop weight W, lb	216
Drop height H, in.	111.4
Number of washers N	76
Dimension "A," in.	9.19
Dimension "B," in.	3.04
Stroke s_1 = A-B, in.	6.15
Dimension "C," in.	19.00
Dimension "D," in.	7.82
Stroke $s_2 - s_1$ = C-D, in.	11.18
Total stroke s_2, in.	17.33
Stroke time t_1, msec	21
Stroke time t_2, msec	104
Washer hardness, R_B number	79
Force F_1, lb	1950
Force F_{min}, lb	1720
Force F_2, lb	2260

(b) Test values.

Figure 17.- Continued.

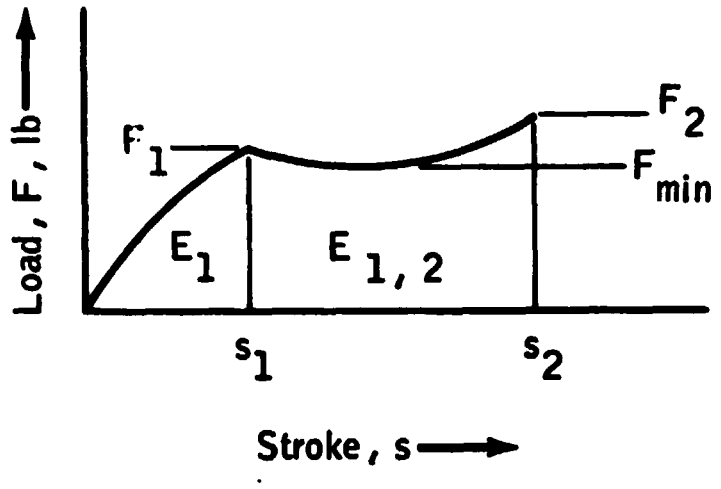

Maximum stroking velocity V_{max}, ft/sec	24.45
Stroke at $V = V_{max}$, in.	0.00
Average stroking velocity $\overline{V} = s_2/t_2$, ft/sec	13.90
Absorbed energy, $0 < s < s_1$, E_1, in-lb	7 248
Average load, $0 < s < s_1$, $\overline{P}$, lb	1 180
Absorbed energy, $s_1 < s < s_2$, $E_{1,2}$, in-lb	20 556
Average load, $s_1 < s < s_2$, $\overline{F}$, lb	1 840
Average load per washer, $\overline{f} = \overline{F}/N$, lb	24.2
Ratio $\overline{P}_t/\overline{F}$, percent	64.1
Ratio $F_1/\overline{F}$, percent	106.0
Ratio $F_{min}/\overline{F}$, percent	93.5
Ratio $F_2/\overline{F}$, percent	122.9

(c) Calculated values.

Figure 17.- Concluded.

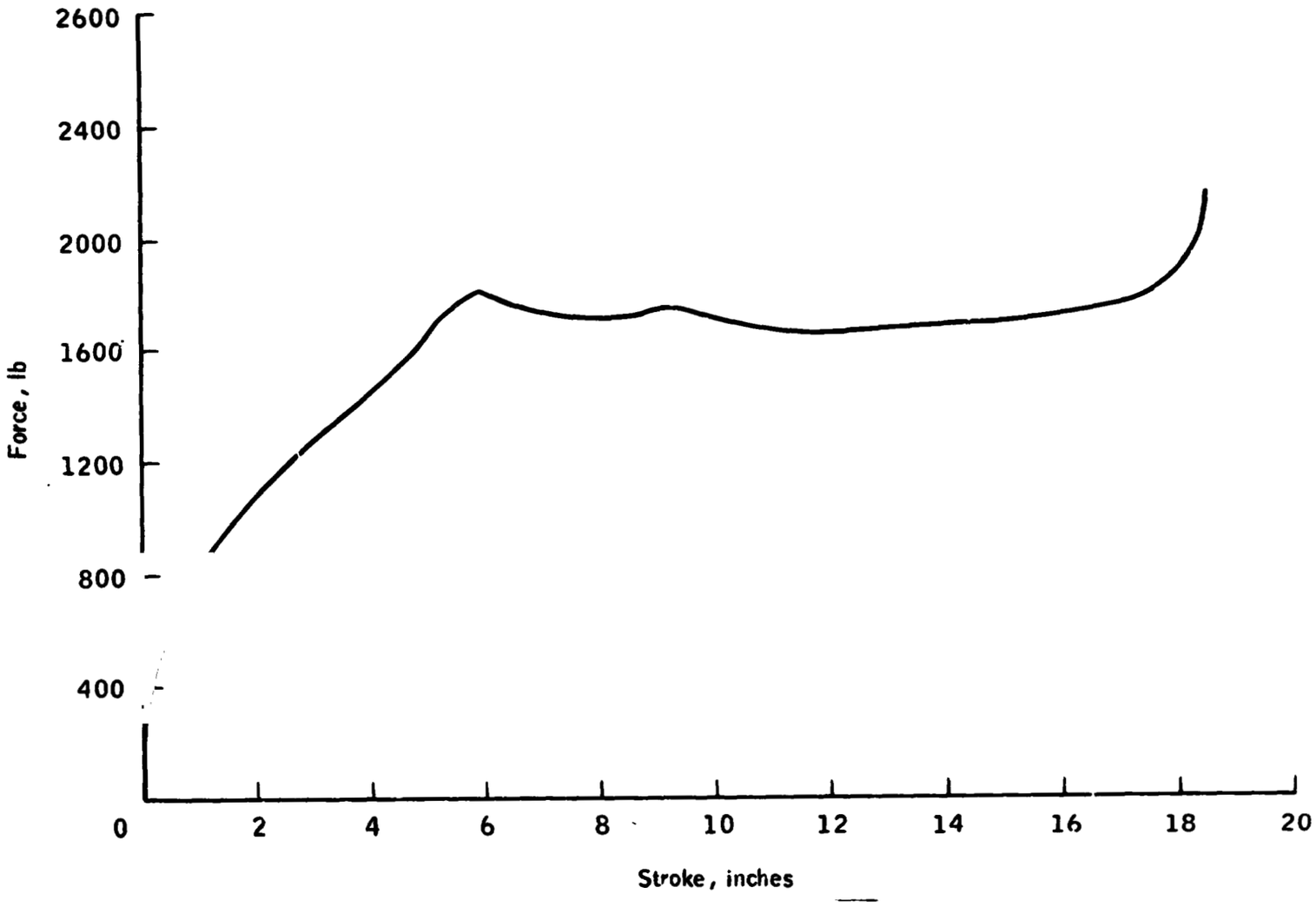

(a) Load-stroke curve.

Figure 18.- Data for test 4B.

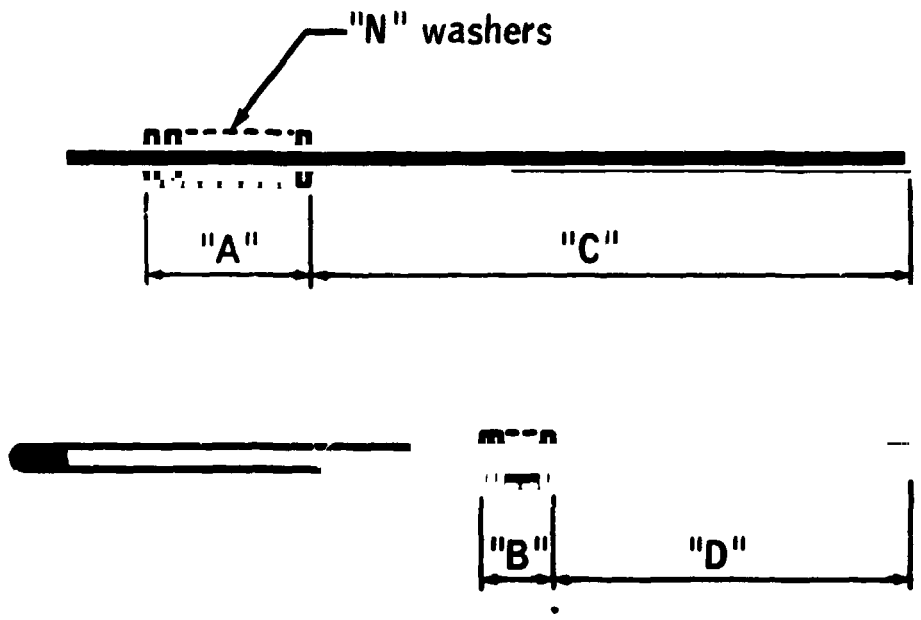

Date of test	12/30/68
Drop rig	B
Rod size, in.	3/8
Drop weight W, lb	144
Drop height H, in.	
Number of washers N	76
Dimension "A," in.	8.92
Dimension "B," in.	3.04
Stroke s_1 = A-B, in.	5.88
Dimension "C," in.	19.00
Dimension "D," in.	6.35
Stroke $s_2 - s_1$ = C-D, in.	12.65
Total stroke s_2, in.	18.53
Stroke time t_1, msec	33
Stroke time t_2, msec	106
Washer hardness, R_B number	76
Force F_1, lb	1760
Force F_{min}, lb	1650
Force F_2, lb	2170

(b) Test values.

Figure 18.- Continued.

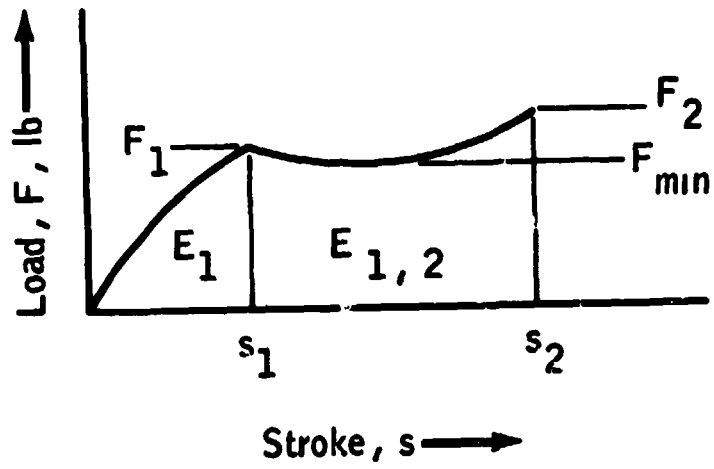

Maximum stroking velocity V_{max}, ft/sec	28.88
Stroke at $V = V_{max}$, in.	4.36
Average stroking velocity $\bar{V} = s_2/t_2$, ft/sec	14.60
Absorbed energy, $0 < s < s_1$, E_1, in-lb	7 220
Average load, $0 < s < s_1$, $\bar{P}$, lb	1 228
Absorbed energy, $s_1 < s < s_2$, $E_{1,2}$, in-lb	21 540
Average load, $s_1 < s < s_2$, $\bar{F}$, lb	1 719
Average load per washer, $\bar{f} = \bar{F}/N$, lb	22.6
Ratio $\bar{P}_t/\bar{F}$, percent	69.8
Ratio $F_1/\bar{F}$, percent	102.3
Ratio $F_{min}/\bar{F}$, percent	95.9
Ratio $F_2/\bar{F}$, percent	126.2

(c) Calculated values.

Figure 18.- Concluded.

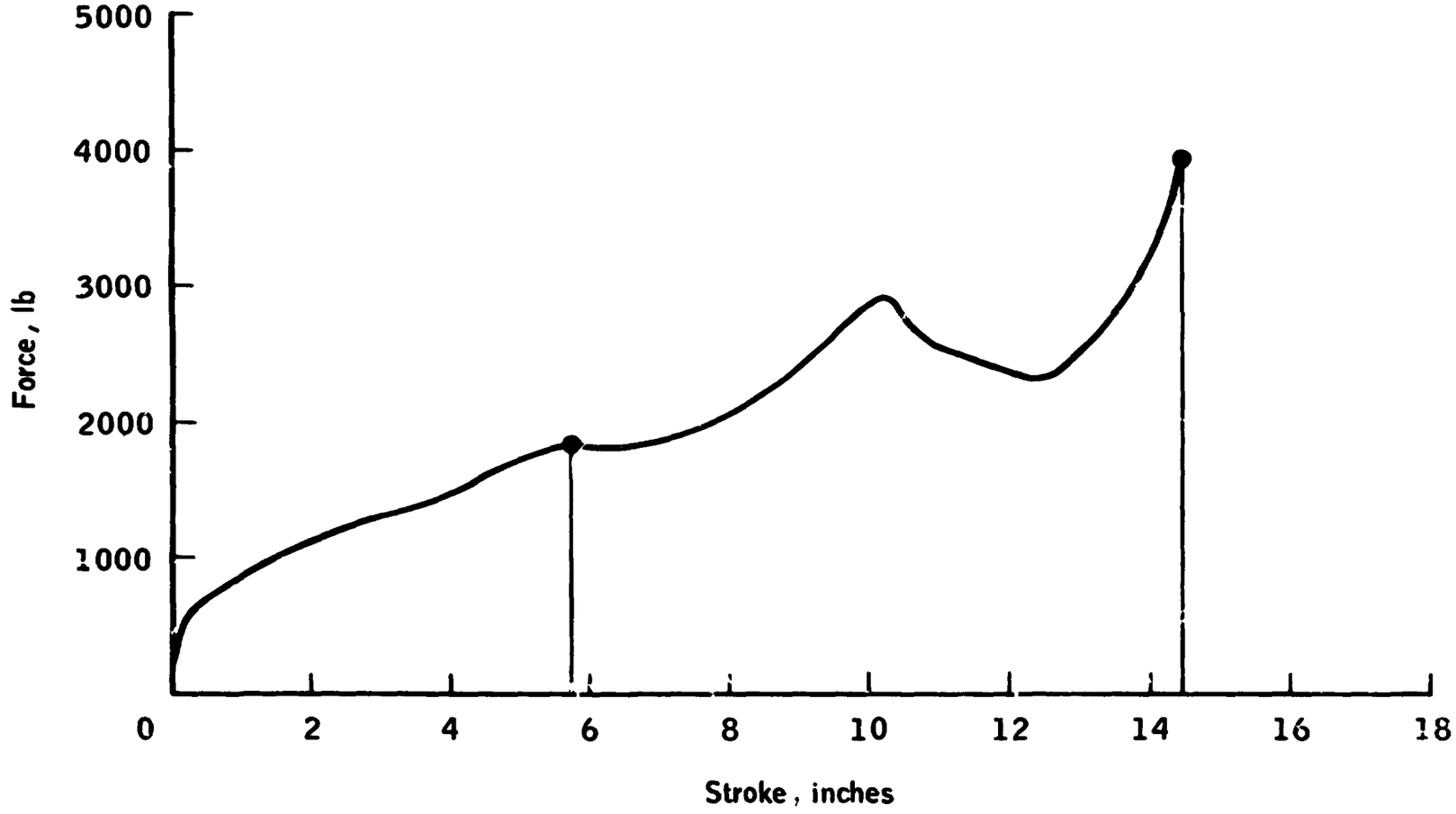

(a) Load-stroke curve.

Figure 19.- Data for test 5B.

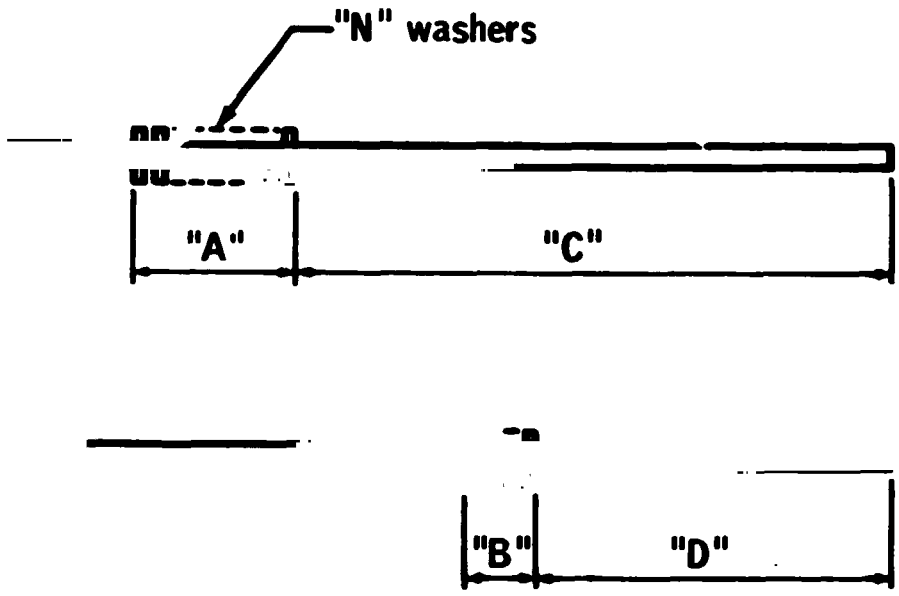

Date of test	1/8/69
Drop rig	B
Rod size, in.	3/8
Drop weight W, lb	144
Drop height H, in.	
Number of washers N	76
Dimension "A," in.	8.95
Dimension "B," in.	3.04
Stroke s_1 = A-B, in.	5.91
Dimension "C," in.	15.33
Dimension "D," in.	6.80
Stroke $s_2 - s_1$ = C-D, in.	8.53
Total stroke s_2, in.	14.44
Stroke time t_1, msec	34
Stroke time t_2, msec	81
Wesher hardness, R_B number	
Force F_1, lb	1830
Force F_{min}, lb	2276
Force F_2, lb	3926

(b) Test values.

Figure 19.- Continued.

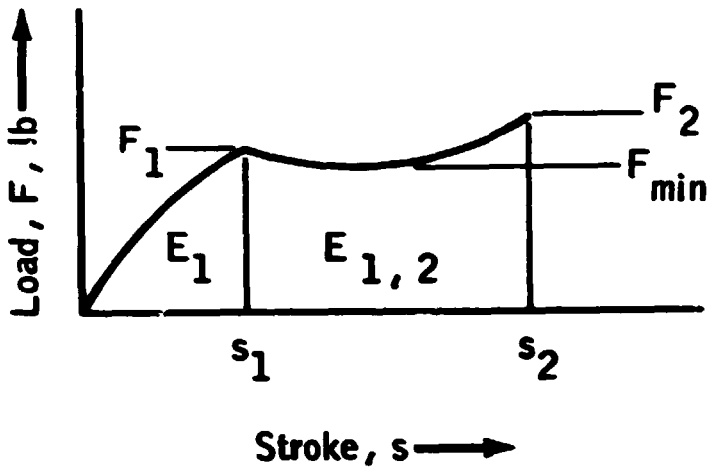

Maximum stroking velocity V_{max}, ft/sec	28.5
Stroke at $V = V_{max}$, in.	4.5
Average stroking velocity $\bar{V} = s_2/t_2$, ft/sec	14.9
Absorbed energy, $0 < s < s_1$, E_1, in-lb	7 500
Average load, $0 < s < s_1$, $\bar{P}$, lb	1 270
Absorbed energy, $s_1 < s < s_2$, $E_{1,2}$, in-lb	20 600
Average load, $s_1 < s < s_2$, $\bar{F}$, lb	2 420
Average load per washer, $\bar{f} = \bar{F}/N$, lb	31.8
Ratio $\bar{P}_t/\bar{F}$, percent	52.5
Ratio $F_1/\bar{F}$, percent	75.7
Ratio $F_{min}/\bar{F}$, percent	94.0
Ratio $F_2/\bar{F}$, percent	162.0

Remarks: This rod and washer assembly was furnished by North American Rockwell. It was received in a "wiped clean" condition. No additional lubricant was applied. Galling occurred on the last 2 inches of stroke, and the washers were canted with respect to the rod.

(c) Calculated values.

Figure 19.- Concluded.

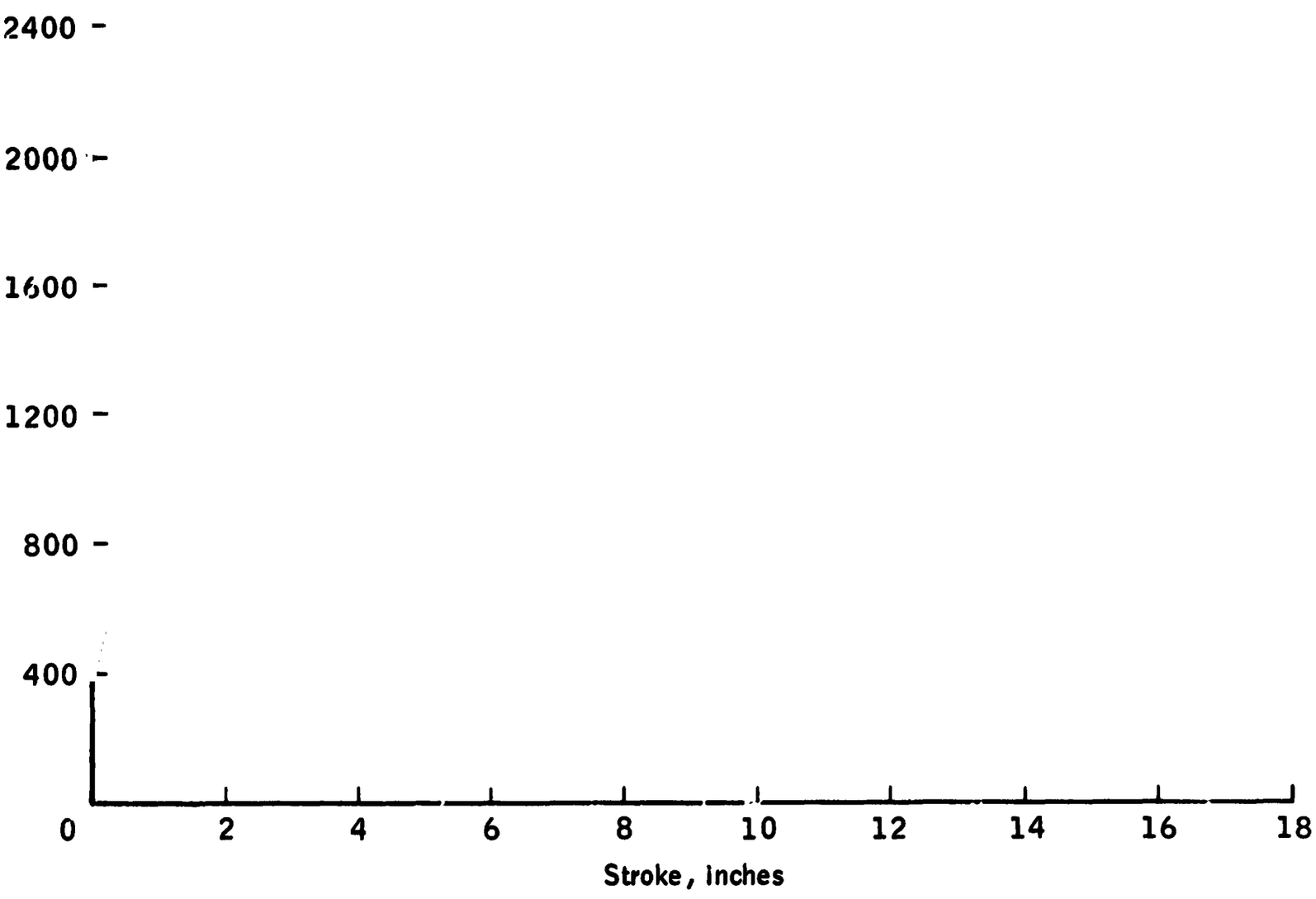

(a) Load-stroke curve.

Figure 20.- Data for test 6B.

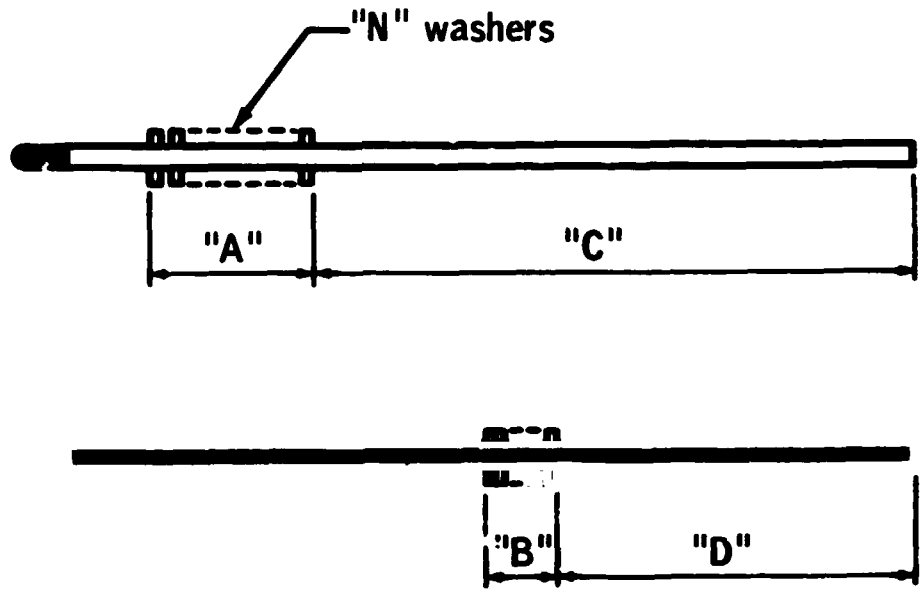

Date of test	1/8/69
Drop rig	B
Rod size, in.	3/8
Drop weight W, lb	144
Drop height H, in.	
Number of washers N	76
Dimension "A," in.	8.95
Dimension "B," in.	3.04
Stroke s_1 = A-B, in.	5.91
Dimension "C," in.	15.37
Dimension "D," in.	3.88
Stroke $s_2 - s_1$ = C-D, in.	11.49
Total stroke s_2, in.	17.40
Stroke time t_1, msec	34
Stroke time t_2, msec	104
Washer hardness, R_B number	
Force F_1, lb	2030
Force F_{min}, lb	1600
Force F_2, lb	2230

(b) Test values.

Figure 20.- Continued.

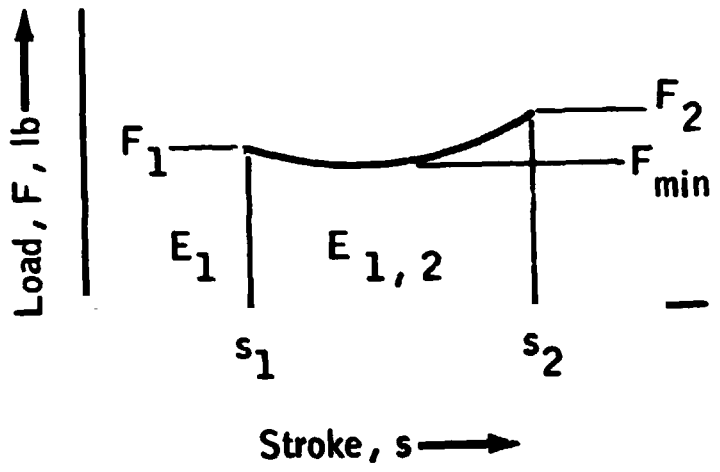

Maximum stroking velocity V_{max}, ft/sec	27.91
Stroke at $V = V_{max}$, in.	4.20
Average stroking velocity $\bar{V} = s_2/t_2$, ft/sec	13.90
Absorbed energy, $0 < s < s_1$, E_1, in-lb	7 860
Average load, $0 < s < s_1$, $\bar{F}$, lb	1 377
Absorbed energy, $s_1 < s < s_2$, $E_{1,2}$, in-lb	20 500
Average load, $s_1 < s < s_2$, $\bar{F}$, lb	1 756
Average load per washer, $\bar{f} = \bar{F}/N$, lb	23.3
Ratio $P_t/\bar{F}$, percent	78.2
Ratio $F_1/\bar{F}$, percent	116.0
Ratio $F_{min}/\bar{F}$, percent	91.4
Ratio $F_2/\bar{F}$, percent	127.5

Remarks: This rod and washer assembly was furnished by North American Rockwell. It was received in a "wiped clean" condition. Prior to installing into test fixture, it was thoroughly resprayed.

(c) Calculated values.

Figure 20.- Concluded.

3. Lubrication MS-122 was liberally applied with the exception of test 5B.

4. Cleanliness at assembly - with the exception of test 45A, the rods and washers were cleaned with Freon prior to assembly, and care was taken not to handle the rods and washers with bare hands.

5. The washer material was 416 stainless steel.

6. The washers were uniformly spaced.

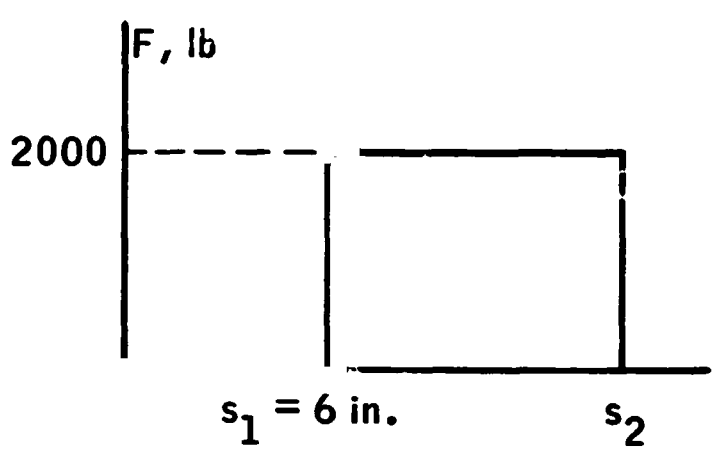

Figure 21.- Desired load-stroke curve.

Notes on the various tests as well as individual load-stroke curves are given in figures 13 to 20. All the load-stroke curves have the same general characteristics. The load per washer starts off high, decreases to a minimum at approximately 75-percent stroke, and then increases sharply toward the end of the stroke. There are two aspects that can account for these characteristics.

1. Expansion and contraction of the washer caused by thermal strains

2. Effects of surface temperature on coefficient of friction

Because of the extremely short stroke time (0.10 second), the bulk of the washer remains relatively cool as compared to the surface temperature that is generated from the large quantity of heat liberated at the

sliding surface. For this reason, the first aspect is believed to have only a minor effect on the resulting load, and the second aspect has a major effect.

In mechanical components such as clutches and brakes, the coefficient of friction is significantly affected by surface temperature. As the temperature builds up, the coefficient of friction decreases with the result that brakes and clutches fade from severe usage.

Examination of figure 12 reveals that, when the acceleration is -7.8g, the surface temperature increases rapidly at the beginning of the stroke, reaches a maximum at approximately 75-percent stroke, and then decreases sharply toward the end of the stroke. This is apparently inverse to the observed load-stroke curves as shown in figure 22.

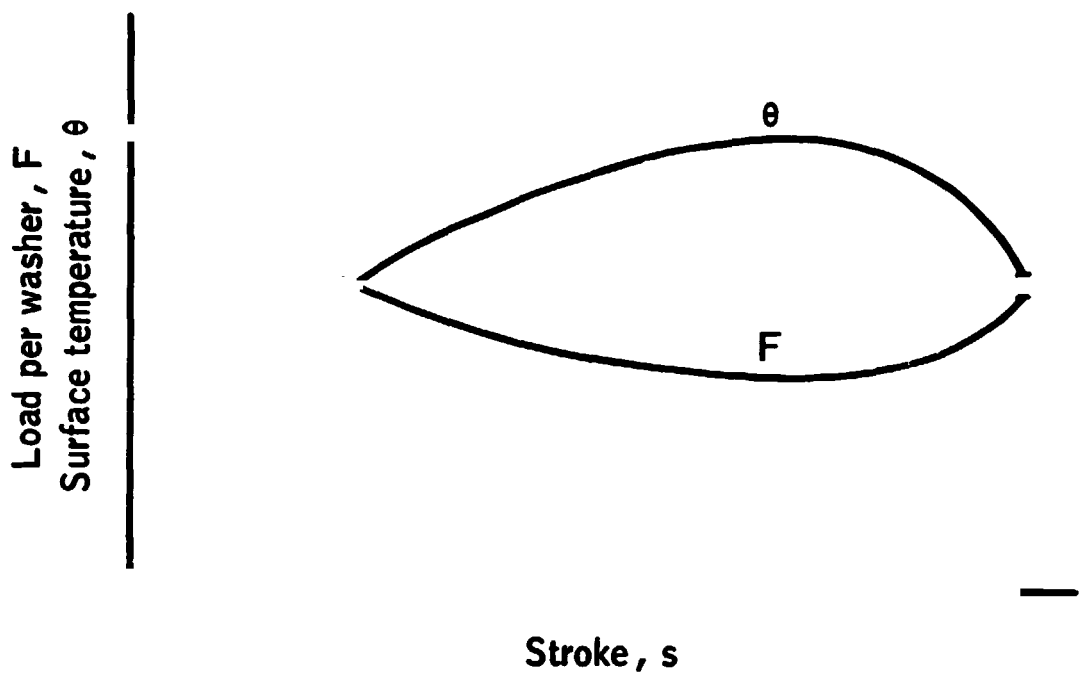

Figure 22.- Characteristic surface temperature and load as a function of stroke.

Washer Load Chart

Examination of the load-stroke curves reveals that the load at a particular displacement or time does not bear a good relationship to the corresponding stroking velocity. Even if such a relationship were

made, it would be difficult to use for future design. A better solution is to set up a relationship between average values such as

$$\overline{f} = \phi(\overline{V}, \text{BHN}) \tag{21}$$

When the results of the valid test data were initially plotted, it became apparent that a linear equation of the form

$$\overline{f} = A(\text{BHN})(1 - B\overline{V}) \tag{22}$$

could be used for the velocity range $10 < \overline{V} < 14$ ft/sec. It was also apparent from the loads necessary to install the washers (at 0^+ velocity) that the curves from equation (22) could be reasonably extrapolated in the velocity range $0 < \overline{V} < 10$ ft/sec. The values A and B are determined from the test data and substituted into equation (22) to obtain

$$\overline{f} = (0.343)(\text{BHN})(1 - 0.0356\overline{V}) \tag{23}$$

The results of this equation are plotted in figure 3.

CONCLUSIONS

The test program has proven that the low onset-rate energy absorber can be used as a workable and reliable energy absorbing system, and the following specific conclusions can be drawn.

1. The average load produced from the rod and washer assembly is predictable if the average velocity is known.

2. The instantaneous load appears to be an inverse function of the surface temperature, which in turn is determined by velocity and acceleration.

3. The best lubricant found was Miller Stephenson MS-122, which is a fluorocarbon dry-film spray-on lubricant.

4. The best material combination found was 718 inconel rods (heat treated to R_C 40) and fully annealed 416 stainless steel washers.

5. The limiting stroking velocity is greater than 28 ft/sec.

6. Other possible rod materials are nickel-plated alloy steel and beryllium copper which has a higher thermal conductivity that permits more heat to pass into the rod.

7. Other possible washer materials are aluminum bronze (10-percent aluminum) and Monel.

8. This device has no known size limitation; however, for weight savings, the rod could be tubular for the larger sizes. A 1/2-inch nominal-size rod and washer assembly was successfully tested, and the results appeared promising; however, the limited number of tests prevents definite conclusions.

9. The energy absorption rate per unit area of contact is about 11 hp/in^2. This value was derived from test data and the following relationship.

$$\text{energy absorption rate per unit area of contact} = \frac{\text{energy under load-stroke curve}}{(\text{stroke time})(\text{area in contact})}$$

This energy absorption rate is indicative of the overall capability of this device and can be used for future design efforts. It could probably be increased by using materials that have a higher thermal conductivity. For comparison purposes, clutches operate in the range of 0.3 to 0.5 hp/in^2.

10. In the limited research and development that was done to solve this one specific problem, no attempt was made to define the limits of this type of system not to define other variations of the system. However, the program did point out a phenomenon that suggests further investigation.

REFERENCES

1. Timoshenko, S.: Strength of Materials. Part II Advanced Theory and Problems, Third ed., D. Van Nostrand Co., Inc., 1956, pp. 386 to 392.

2. Roark, Raymond J.: Formulas for Stress and Strain. Third ed., McGraw-Hill Book Co., Inc., 1954, p. 276.

3. Rothbart, Harold A.: Mechanical Design and Systems Handbook. McGraw-Hill Book Co., Inc., 1964, pp. 28-8 to 28-11.